MANUFACTURING OF STARCH-BASED BIOPLASTIC FROM WASTE POTATO STARCH BY EXTRUSION AND ENERGY ANALYSIS OF THE PRODUCTION

A Thesis Submitted to
the Graduate School of Engineering and Sciences of
İzmir Institute of Technology
in Partial Fulfillment of the Requirements for the Degree of

MASTER OF SCIENCE

in Energy Engineering

by
Yasemin GÖKYILDIZ

September 2023
İZMİR

We approve the thesis of **Yasemin GÖKYILDIZ**

Examining Committee Members:

Prof. Dr. Ahmet YEMENİCİOĞLU
Food Engineering, Izmir Institute of Technology

Assoc. Dr. Aylin ZİYLAN
Metallurgy and Materials Engineering, Dokuz Eylül University

Assoc. Dr. Nilay GİZLİ
Chemical Engineering, Ege University

20/09/2023

Prof. Dr. Sacide ALSOY ALTINKAYA
Supervisor, Chemical Engineering
Izmir Institute of Technology

Prof. Dr. Funda TIHMINLIOĞLU
Co-Supervisor, Chemical Engineering
Izmir Institute of Technology

Prof. Dr. Gülden Gökçen AKKURT
Head of the Department of Energy Systems Engineering

Prof. Dr. Mehtap EANES
Head of the Graduate School of Engineering and Sciences

ACKNOWLEDGMENTS

I would like to express my special thanks to my supervisor, Prof. Dr. Sacide ALSOY ALTINKAYA and my co-supervisor, Prof. Dr. Funda TIHMINLIOĞLU for their guidance, support, encouragement, and insightful comments during the progress of my master's thesis.

I am also thankful to the rest of my thesis defense committee, Prof. Dr. Ahmet YEMENİCİOĞLU, Assoc. Dr. Aylin ZİYLAN and Assoc. Dr. Nilay GİZLİ for their valuable comments and contributions.

I would like to thank ILGINLAR Industrial Food Recovery and Feed Raw Materials Logistics Industry Trade Inc. and the members of the research and development laboratory, Prof. Dr. Behzat GÜRKAN and Dilan GÜNCÜ for their guidance and support.

I would like to express my genuine thanks to my family and friends, my mother Hülya ERDEM, my sister Yeliz GÖKYILDIZ, my friend Seyra TOPRAK and my love Burak ERÇELİK for always believing in me, supporting me and being by my side.

ABSTRACT

MANUFACTURING OF STARCH-BASED BIOPLASTIC FROM WASTE POTATO STARCH BY EXTRUSION AND ENERGY ANALYSIS OF THE PRODUCTION

Plastic materials are an essential part of our daily lives and annual production is higher than 380 million tons with a 4% increasing rate. Since the 1950s, 8.3 billion tons of plastic have been produced, 9% of these plastics have been recycled, 12% have been incinerated and the rest 79% have been dumped to landfills. Therefore, the development of biobased and biodegradable polymers has become a priority to reduce the environmental impact and dependency on fossil resources. Thermoplastic starch (TPS) is a starch-based bioplastic obtained by the disruption of the starch granules with thermal and mechanical forces in the presence of plasticizer. In this thesis, production of TPS from residual potato starch by extrusion was investigated. Glycerol was selected as plasticizer and added to starch with 20, 30 and 40 wt.%. Extrusion temperature profiles were selected as 50-90ºC, 60-90ºC and 70-90ºC. The pretreatment conditions for the residual starch were drying to 10 wt.% moisture content and sieving with 131µm mesh size. Specific mechanical energy values ranged between 7.89 $kWhkg^{-1}$ and 43.27 $kWhkg^{-1}$. The optimum product formation was selected according to processability with lower energy consumption and mechanical properties as TPS303 which has 30 wt.% glycerol content and processed between 70-90ºC. Specific mechanical energy consumption for TPS303 was found to be 23.78 $kWhkg^{-1}$. The mechanical properties of TPS303 were 4.48 MPa tensile strength, 59.74 MPa Young's modulus and 57.33% elongation at break. Consequently, residual potato starch was found to be a promising raw material for thermoplastic starch production with proper pretreatment.

ÖZET

ATIK PATATES NİŞASTASINDAN EKSTRÜZYONLA NİŞASTA BAZLI BİYOPLASTİK ÜRETİMİ VE SİSTEMİN ENERJİ ANALİZİ

Plastik malzemeler günlük hayatımızın vazgeçilmez bir parçasıdır ve plastik üretimi yıllık %4 artış oranıyla 380 milyon ton/yılın üzerindedir. 1950'lerden bu yana 8,3 milyar ton plastik üretilmiş, bu plastiklerin %9'u geri dönüştürülürken %12'si yakılmış ve geri kalan %79'u sahalara atılmıştır. Bu nedenle, biyobazlı ve biyolojik olarak parçalanabilen polimerlerin geliştirilmesi, çevresel etkiyi ve fosil kaynaklara bağımlılığı azaltmak için bir öncelik haline gelmiştir. Termoplastik nişasta (TPS), nişasta granüllerinin plastikleştirici varlığında termal ve mekanik kuvvetlerle parçalanmasıyla elde edilen nişasta bazlı bir biyoplastiktir. Bu tezde, ekstrüzyon ile artık patates nişastasından TPS üretimi incelenmiştir. Plastikleştirici olarak gliserol seçilmiş ve nişastaya ağırlıkça %20, %30 ve %40 oranlarında eklenmiştir. Ekstrüzyon sıcaklık profilleri 50-90^{o}C, 60-90^{o}C ve 70-90^{o}C olarak belirlenmiştir. Kalıntı nişasta için ön işlem koşulları, ağırlıkça %10 nem içeriğine kadar kurutma ve 131µm gözenek boyutunda eleme olarak seçilmiştir. Spesifik mekanik enerji tüketimi değerleri 7,89 kWhkg^{-1} ile 43,27 kWhkg^{-1} arasında hesaplanmıştır. Optimum ürün uygun mekanik özellikler ve düşük enerji tüketimli işlenebilirliği ile TPS303 kodlu ürün olarak seçilmiştir. Ağırlıkça %30 gliserol içeren TPS303, 70-90^{o}C sıcaklıkları arasında işlenmiştir. TPS303 için spesifik mekanik enerji tüketimi 23,78 kWhkg^{-1} olarak bulunmuştur. TPS303'ün çekme mukavemeti 4,48 MPa, Young modülü 59,74 MPa ve kopma uzaması %57,33 olarak belirlenmiştir. Sonuç olarak, kalıntı patates nişastasının uygun ön işlemle termoplastik nişasta üretimi için umut verici bir hammadde olduğu bulunmuştur.

TABLE OF CONTENT

LIST OF FIGURES

Figure **Page**

LIST OF TABLES

Table **Page**

CHAPTER 1

INTRODUCTION

Plastics are fossil-fuel derived synthetic polymers that are an essential part of our daily lives with many favorable properties such as low cost, lightweight, easy processability, etc. Plastic materials are primarily used in packaging, electrical and electronics, building and construction, transport, and agriculture. (Laftah, 2017). The annual plastic production has been estimated to be higher than 380 million tons, and the rate is increasing by 4% yearly (Rosenboom et al., 2022).

With large production and consumption rates, plastic pollution has become a global concern due to the mismanagement of the generated waste. 8.3 billion tons of plastics have been produced since the 1950's. 9% of these plastics have been recycled, 12% have been incinerated and rest 79% have been dumped into landfills (Rosenboom et al., 2022). In the marine environment, plastics degrade into smaller particles, called microplastics. Microplastics are less than 5 mm in diameter and cause health problems in living organisms by entering the food chain. Due to the particulate nature of microplastics, they could spread contaminants by absorbing and carrying them (Ziccardi et al., 2016). Since the current plastic economy works linearly by extracting fossil resources and creating pollution by mismanagement of waste, a circular plastic economy is required for a sustainable future. Accordingly, bioplastics arouse interest as an alternative to conventional petroleum-based plastics.

According to the definition of European Bioplastics, if the plastic material is biobased, biodegradable or both, it is defined as bioplastic. Biobased plastic means that the material is produced from biomass such as corn, sugarcane, cellulose, starch etc. Biodegradable plastic means that the plastic material can be converted to natural substances such as water, carbon dioxide and compost by microorganisms in the natural environment. The annual production of biobased plastics was estimated to be nearly 2 million tons. Nowadays, the main raw materials for bioplastics are crops. The current speculations around bioplastic production from agricultural feedstocks address the competition between food production for land area and fresh water. Therefore,

agricultural, or other waste materials and microalgae as raw materials are considered a more sustainable approach (Karan et al., 2019).

Starch is a natural biopolymer produced in plants such as corn, wheat, potato, barley, etc. The renewability, low cost, and abundance make starch an advantageous feedstock for bioplastic production; however, the food scarcity problem interrogates using a food source as a plastic feedstock. Thermoplastic starch (TPS) is a starch-based bioplastic obtained by the disrupting starch granule with thermal and mechanical forces in the presence of a plasticizer (Halley & Dorgan, 2011). The typical production methods for TPS production are extrusion, kneading, casting, and injection or blow molding. Extrusion is the most common method for TPS production since it allows continuous production (Singh & Genovese, 2021).

The circular economy concept suggests industrial systems close loops by reducing waste formation and minimizing energy and feedstock consumption (Dobrucka, 2019). The amount of CO_2 released into the atmosphere from plastics manufacturing was estimated to be nearly 850 million tons, accounting for 2% of global CO_2 emissions in 2019 (Rosenboom et al., 2022). A significant part of CO_2 emissions in the plastic industry was related to the extraction of raw materials and manufacturing of polymers. Therefore, practical methods for plastic production that minimize the unit energy consumption need to be further evaluated by considering raw material selections (Schulze et al., 2017).

The Sustainable Development Goal 12 of the United Nations suggests lowering the formation of global food waste through the Responsible Consumption and Production Act (Charles et al., 2022). There is a potential residual starch formation from potato chip production firms which could be further utilized as thermoplastic starch. In the potato chip production process, washing and cutting the potatoes creates a wastewater stream that is high in starch concentration. The starch is further separated from wastewater by a decanter centrifuge. The residual starch arriving at Ilgınlar Industrial Food Waste Recovery company is estimated to be nearly 1,500 tons annually.

In this thesis, the production of thermoplastic starch from the residual potato starch by extrusion was studied. Optimum process temperature and glycerol content were selected based on specific mechanical energy consumption and applicable mechanical properties. Utilizing residual starch for thermoplastic starch production was considered as an innovative approach with the utilization of food waste in parallel with the Goal 12

of The Sustainable Development Goals. The source of potato starch was the production lines of potato chips. The pretreatment of the starch was conducted by lowering the moisture content from 40 to 10 wt.% and sieving with 131μm mesh sizes. The pretreated potato starch was extruded in a single-screw extruder with using glycerol as plasticizer. Different glycerol contents and temperature profiles were studied. Different pretreatment conditions for the residual potato starch were studied by drying to 10 and 26 wt.% moisture contents and sieving with 131μm and 300μm mesh sizes. Specific mechanical energy consumption was calculated for each of the trials. Mechanical testing was conducted for the obtained extrudates. Also, XRD analysis was conducted to study the structure of the thermoplastic starches.

CHAPTER 2

LITERATURE REVIEW

2.1. Bioplastics

Bioplastics are a group of polymers with various qualities and applications. European Plastics categorizes bioplastics in three main titles: biobased plastics, biodegradable plastics and both bio-based and bio-degradable plastics. Therefore, the raw material and biodegradability are two major characteristics for defining plastic materials (Jõgi & Bhat, 2020). Fig. 2.1., the plastic categorization where the bioplastics were labeled with a green leaf symbol. Since bioplastics could be produced from renewable resources, they are considered more sustainable alternatives to fossil-based and non-biodegradable plastics. In 2022, the most used bioplastic polymers are PLA (polylactic acid), starch blends, bio-PE (bio-polyethylene) and bio-PTT (bio-polytrimethylene terephthalate) (European Bioplastics, 2022).

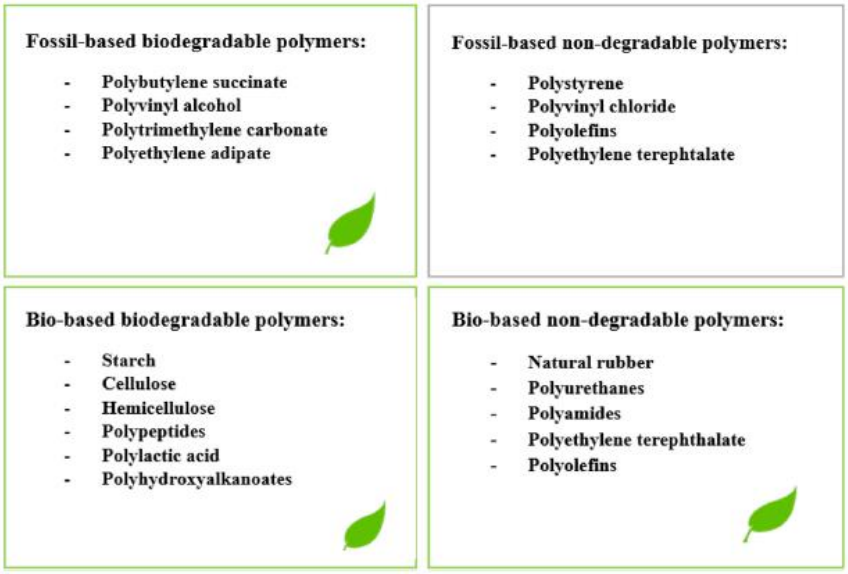

Figure 2.1. Classification of plastic types depending on raw material and biodegradability (Jõgi & Bhat, 2020).

Depending on material features, bioplastics could be further categorized as thermoplastics and thermosets. Thermoplastics could be heated and cooled in reverse for

a limited amount without affecting the structure or material properties such as color, shape, and microstructural alteration, etc. On the contrary, thermosets' heating and solidification process is irreversible resulting in chemical decomposition and structural change. Also, mechanical properties such as hardness, tensile strength, etc., are temperature-dependent for thermoplastics but not for thermosets (Bîrca et al., 2019).

Plastic material is considered biodegradable if the biological activity of microorganisms such as bacteria, archaea, fungi etc., could completely degrade the plastic. When the plastic material is degraded under aerobic conditions, it turns into biomass, carbon dioxide and water. However, under anaerobic conditions, the plastic material degrades into biomass, carbon dioxide, water, and methane (Dilkes-Hoffman et al., 2019).The physico-chemical structure of plastic polymer affects its biodegradability. Also, biodegradability highly depends on environmental factors such as temperature, moisture, pH, etc. (Emadian et al., 2017). If the plastic material is biodegradable under composting conditions within 6-12 weeks, it is considered compostable as described by European standard EN 13432 (Jõgi & Bhat, 2020).

According to European Bioplastics, the current global bioplastic production capacity was estimated at 2,2 million tons in 2022. Fig. 2.2. shows global bioplastic production capacities from 2021 to 2027. The bio-based and non-biodegradable parts account for 49%, while the biodegradable part accounts for 51% of the current capacity. Since the demand is constantly increasing, the global production capacity is expected to rise approximately to 6,3 million tons in 2027 (European Bioplastics, 2022).

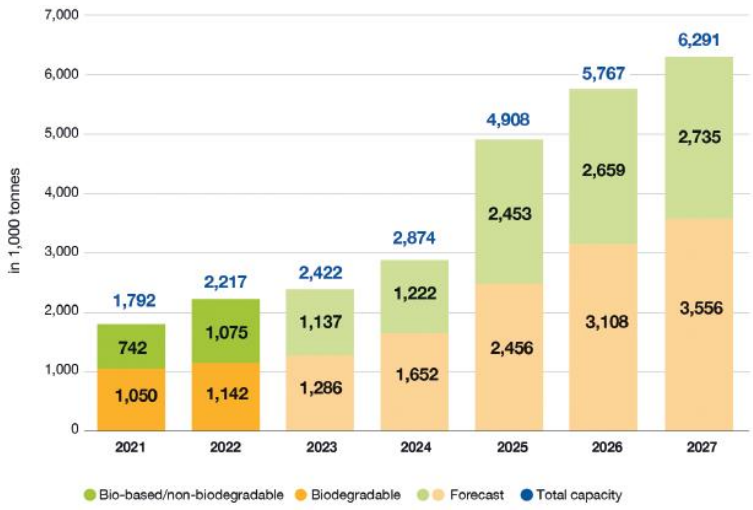

Figure 2.2. Global bioplastic production capacities (European Bioplastics, 2022).

Starch, polylactide, polyhydroxyalkanoates, cellulose, lignin-based packaging materials are some of the recently developed polymers currently available on the market (Dobrucka, 2019). Fig. 2.3. shows global bioplastic production capacities by market segments in 2022. Bioplastics have been utilized in various sectors, mainly as packaging, fibers, consumer goods, automotive, etc. The packacing sector has the most bioplastics utilization among other market segments in 2022 (European Bioplastics, 2022).

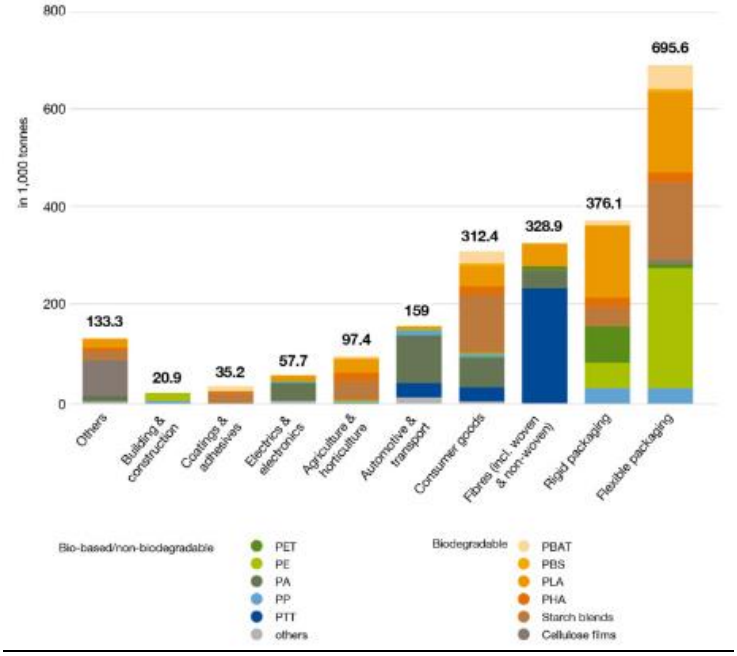

Figure 2.3. Global bioplastic production capacities by market segments in 2022 (European Bioplastics, 2022).

Growing renewable raw materials for bioplastic production accounts for approximately 0.015% of the global agriculture area which is 0.8 million hectares in 2022. The forecast land use for bioplastic production is expected to increase to 0.06% which is 2,9 million hectares in 2027 (European Bioplastics, 2022). This land share was considered applicable for certain opinions; however, speculations about the competition between agricultural land use and bioplastic production continues. Next generation bioplastic raw materials were expected to be based on microalgae and agricultural waste to eliminate the global land competition.

The end-of-life treatment options for bioplastics include various options such as anaerobic digestion, composting, waste-to-energy, recycling, and landfilling (Song et al., 2009). In Fig. 2.4., the circular waste management strategy was suggested for starch-based bioplastic with composting. Even though biodegradable plastics degrade in the

natural environment without creating toxic effects, the created waste still requires applicable management to develop a circular economy. Both composting and anaerobic digestion are considered practical management strategies since they utilize the waste in another form.

Figure 2.4. Waste management strategy for starch-based bioplastics (BIOTEC, 2023).

2.2. Starch

As a renewable resource, starch is a biodegradable polysaccharide made up of carbon, hydrogen, and oxygen with a $C_6H_{12}O_5$ chemical formula. It occurs as granules in plants such as corn, potato, rice, wheat, maize, tapioca, etc. with 2 to 100μm diameter. Tiny starch granules form in the plant leaves during photosynthesizing in the presence of water, carbon dioxide, and sunlight (Laftah, 2017). The shape and size of the granules depend on the source of starch. The chemical composition of starch granules is 10-29% moisture by weight and trace amounts of proteins, lipids, ash, and inorganic materials (Hoover, 2001).

The granular starch comprises linear amylose and branched amylopectin with typically 20–25 wt.% of amylose and 75–80 wt.% of amylopectin in ratio. Amylose is a polymer chain made up of approximately 6000 glucose units connected with α (1,4) linkages in linear form. Amylopectin is a branched polymer chain connected with α (1,6) linkages with an average of 9600 - 15900 degree of polymerization. The chemical structure of amylose and amylopectin are shown in Fig. 2.5. The Amylose to amylopectin ratio determines the degree of crystallinity in starch, which affects properties such as

solubility, mechanical strength, etc. The amorphous part of the starch granule is formed by amylose and amylopectin branching point, whereas amylopectin short chains form the crystalline part. Starch biodegradation occurs by the activity of microorganisms and enzymes forming carbon dioxide and water (Cazón et al., 2017).

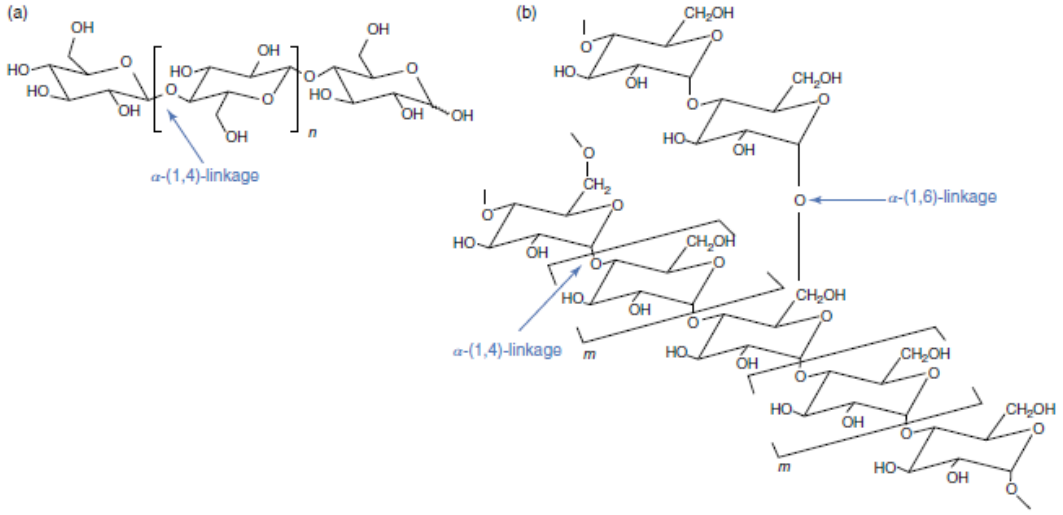

Figure 2.5. Amylose (a) and amylopectin (b) chemical structure (Singh & Genovese, 2021).

Starch granules are insoluble in water below their gelatinization temperature. Interaction between the water molecules and the hydroxyl group of amylose and amylopectin causes starch's partial solubilization when treated with hot water (Cazón et al., 2017). Disruption of the starch granules occurs by the gelatinization process and the gelatinization temperature depends on the source of starch which ranges between 50 to 92ºC. Gelatinization occurs by heating starch granules in the presence of plasticizer as an irreversible process. It causes swelling of starch granules and drives a transition process. Steps of gelatinization involve hydration and solvent diffusion into granules followed by starch crystals melting (Choi et al., 2008). In the case of potato starch, the initial gelatinization temperature varies between 45ºC - 60ºC depending on the potato type (Lizarazo H. et al., 2015).

Since starch is a low-cost, biodegradable, and renewable resource, it is used to produce many materials such as plastics, textiles, papers, and adhesives, etc. and utilized as filler and thickening agent in the pharmaceutical and cosmetic industries (Laftah, 2017). Nowadays, starch is proposed as packaging material to replace fossil-based

packaging with a renewable approach (Singh & Genovese, 2021). Good oxygen properties related with tightly packed and ordered hydrogen bond structures of amylose and amylopectin make starch an attractive packaging material (Mali et al., 2005). Fig. 2.6. shows different technologies for producing starch-based plastics with commercial product names.

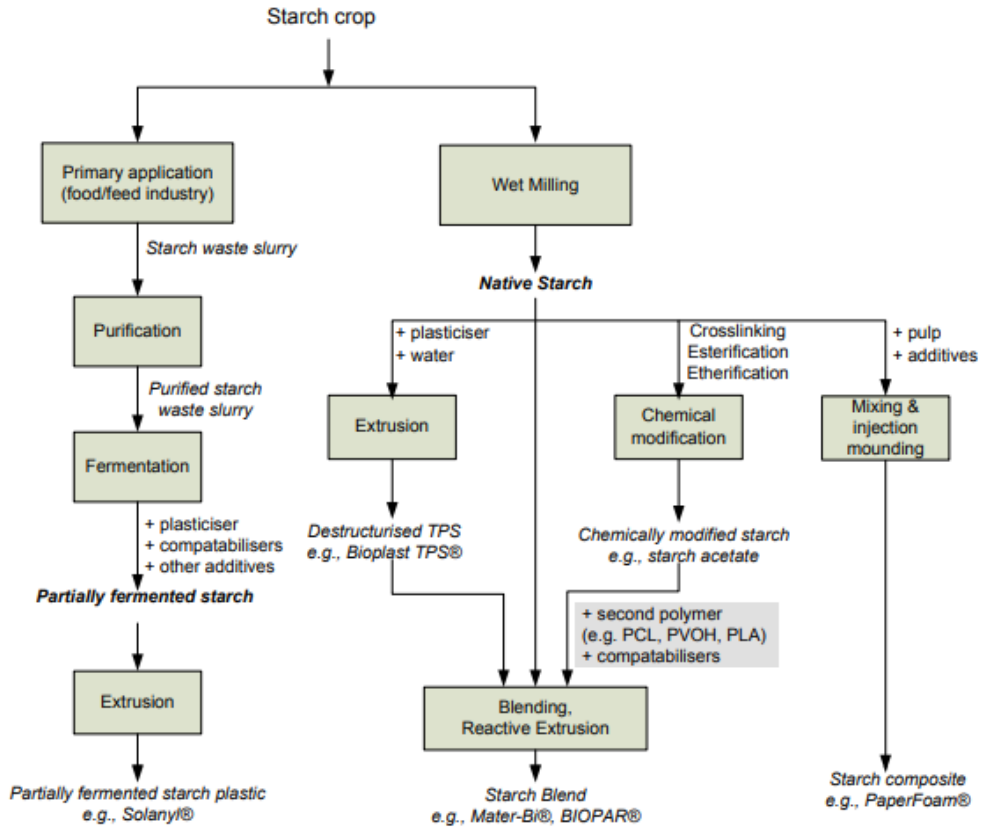

Figure 2.6. Production technologies for starch-based plastics (Shen et al., 2009).

2.3. Thermoplastic Starch (TPS)

Thermoplastic starch (TPS) is a starch-based bioplastic that is obtained by disrupting the crystalline structure of starch granules with thermal and mechanical forces in the presence of a plasticizer. Disruption is generally achieved with the effect of temperature and mechanical forces, resulting in the formation of polymer phase in continuous form. Shopping bags, garbage bags, consumer goods packaging, disposable utensils (straw, fork, spoon, plate etc.), toys, mulch film, etc. are some products that could be produced from TPS. Fig. 2.7. shows the TPS packaging application as an example.

Figure 2.7. Thermoplastic starch packaging application (Halley & Dorgan, 2011).

The production of thermoplastic starch starts with mixing starch with various types of plasticizers such as glycerol, sorbitol, etc. and then processing the mixture via multiple techniques such as extrusion, injection molding and kneading (Zhang et al., 2014). Physical and chemical reactions in TPS production were investigated as diffusion of water, granules expansion, gelatinization, melting, and crystallization (Khan et al., 2016). The features of the final product depend mainly on the amylose to amylopectin ratio of starch, processing methods, processing parameters, and type and concentration of plasticizer (Mali et al., 2005).

Thermoplastic starch is generally produced from corn, potato, and wheat starch. Its formulation varies between 50-90 wt.% starch, 10-50 wt.% plasticizer and fillers with various proportions. Low molecular weight plasticizers occupy the intermolecular spaces between polymer chains increasing macromolecular chains' mobility. Different additives such as plant fibers, emulsifiers, cellulose, etc. were studied to improve the mechanical properties of thermoplastic starch (Forssella et al., 1997). The general mechanical properties of the TPS are shown in Table 2.1.

Table 2.1. The mechanical properties of thermoplastic starches (Hazar Yoruç & Uğraşkan, 2017).

Properties	Density (g/cm^3)	Tensile Strength (MPa)	Elastic Modulus (MPa)	Elongation at Break (%)
TPS	1.0-1.39	5-6	125-850	31-44

Thermoplastic starch is gaining more attention with the current plastic pollution crisis since it is bio-based and biodegradable. Its viscoelastic behavior and physicochemical properties are similar to petroleum-based polymers. Also, their non-toxic, and biodegradable structure makes them a better alternative to synthetic polymers. TPS could be utilized by itself as well as by mixing with various other polymer types such as polyethylene (PE), polystyrene (PS) and polypropylene (PP) to improve mechanical properties and water resistance (Khan et al., 2016). Even though TPS shows good mechanical properties as a renewable plastic material, the main disadvantages are water sensitivity and unsatisfactory product performance in wet or dry environments (Mohammadi Nafchi et al., 2013). Therefore, further studies on increasing the product quality of TPS are frequently studied with additives and processing and blending with other polymers.

2.4. Plasticizers

Plasticizers are materials that increase the flexibility and strength of the plastic material by decreasing the glass transition temperature. Glass transition temperature (T_g) is defined as the temperature at which polymer transits from a glassy state to a rubbery state. Glass transition temperature highly affects the mechanical properties of the material. High glass transition temperature causes brittleness in the material (De Graaf et al., 2003). The effect of glycerol content on the glass transition temperature of thermoplastic starch is shown in Fig. 2.8. According to Fig. 2.8, increasing glycerol content from 15 to 30% decreased the T_g from 130 to 20^{o}C.

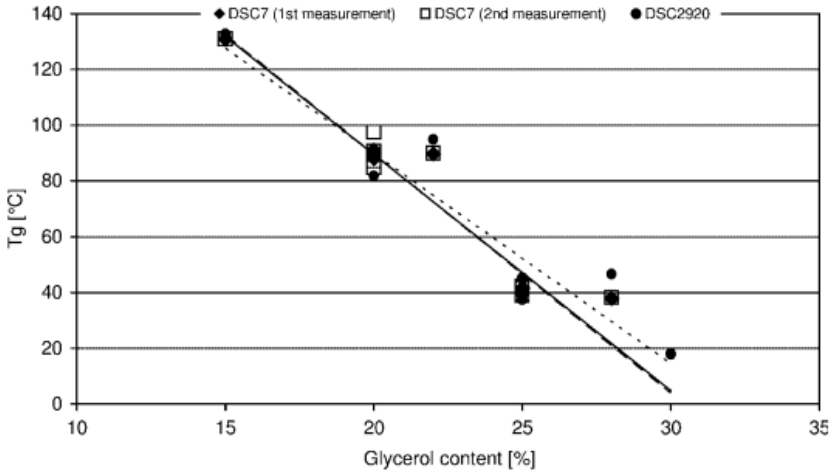

Figure 2.8. Effect of glycerol content on Tg of thermoplastic starch (Janssen & Moscicki, 2009).

Plasticizers have low molecular weights, which makes processing easier. They lower processing temperature by filling the spaces between polymer chains. When the plasticizer penetrates the material, the average molecular weight of the material decreases and more branch structures form (Montilla-Buitrago et al., 2021). Plasticizer added into starch breaks inner hydrogen bonds by replacing the interaction between starch molecules through hydrogen bond formation between polar groups of the plasticizer and hydroxyl groups in the glucose units of the starch. Consequently, the mobility of macromolecules increases, and starch turns into a thermoplastic form (Singh & Genovese, 2021). Fig. 2.9. shows the interactions between starch-glycerol and starch-sorbitol.

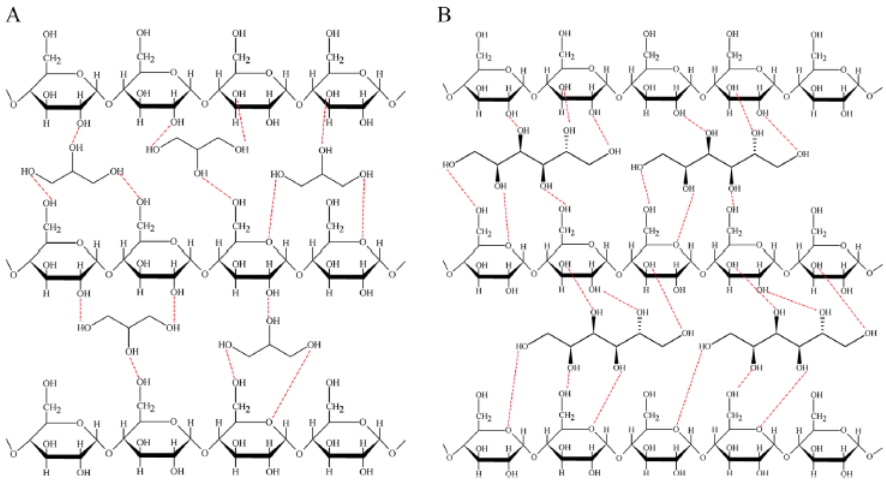

Figure 2.9. Starch–glycerol (A) and starch–sorbitol (B) interaction (Montilla-Buitrago et al., 2021).

Water, which also exists as moisture in initial starch, acts as a plasticizer for starch. However, undesirable bubble formation limits the upper temperature in processing starch. Therefore, water is generally used by mixing with other plasticizers. Commonly used plasticizers for starch are glycerol, sorbitol, ethylene glycol, glucose, fructose, maltodextrin, urea, citric acid, amino acids etc. (Singh & Genovese, 2021). According to advantages such as high boiling point, inexpensiveness and readily available, glycerol is the most used plasticizer in thermoplastic starch production (Kaseem et al., 2012). The concentration of the plasticizer is critical in the plasticization process. Low amounts of plasticizer could prevent plasticization whereas high doses of plasticizer could cause undesirable mechanical properties in thermoplastic starch. For example, adding more than 25-35 wt.% of glycerol causes exudation. Until today, glycerol concentrations were mainly studied between 15 to 30 wt.% by starch dry mass (Singh & Genovese, 2021).

2.4.1. Glycerol

Glycerol, also known as glycerin, is a simple triol with a chemical formula of $C_3H_8O_3$. All natural fats and oils contain glycerol as fatty esters. It is in the form of colorless odorless viscous liquid at room temperature. At atmospheric pressure, glycerol has a boiling point of 290°C. The density of glycerol was estimated as 1.261 g/ml at 20°C. Fats and oils contain glycerol as triglycerides which varies between 8 to 14 wt.% depending on the source (Christoph et al., 2006). In converting fats and oils into fatty acids or fatty acid methyl esters, glycerol forms as a by-product known as natural glycerol. Other synthetic production methods are less common than natural glycerol production, which covers 10% of the total production (Christoph et al., 2006). Various application areas for glycerol are foods, cosmetics, plastics, pharmaceuticals, etc. The annual glycerol production was expected to reach 1700 thousand tons in 2030 (ChemAnalyst, 2020).

2.5. Extrusion

TPS is produced with injection molding, compression molding, film casting, internal mixing, and extrusion. Casting is a common technique to produce starch-based plastics. However, casting takes a long production time and produces limited amounts, therefore it is not considered a feasible process on an industrial scale (González-Seligra et al., 2017). Among other production processes, extrusion allows large-scale continuous TPS production in the form of film, pellets, and sheets (Xie, Luckman, et al., 2014). Other advantages of the extrusion process are high mixing capacity, flexible operation, and low infrastructure (Ochoa-Yepes et al., 2019).

Starch is extruded via a single-screw extruder or a twin-screw extruder. Even though the single-screw extruders provide the advantage of processing high-viscosity starch mixture due to continuous metering, twin-screw extruders are more frequently preferred for their benefit of self-wiping. Also, a twin-screw extruder provides more operational flexibility, which is beneficial for mixing the mixture (Xie et al., 2014). Fig. 2.10. shows the schematic of a twin-screw extruder for TPS production.

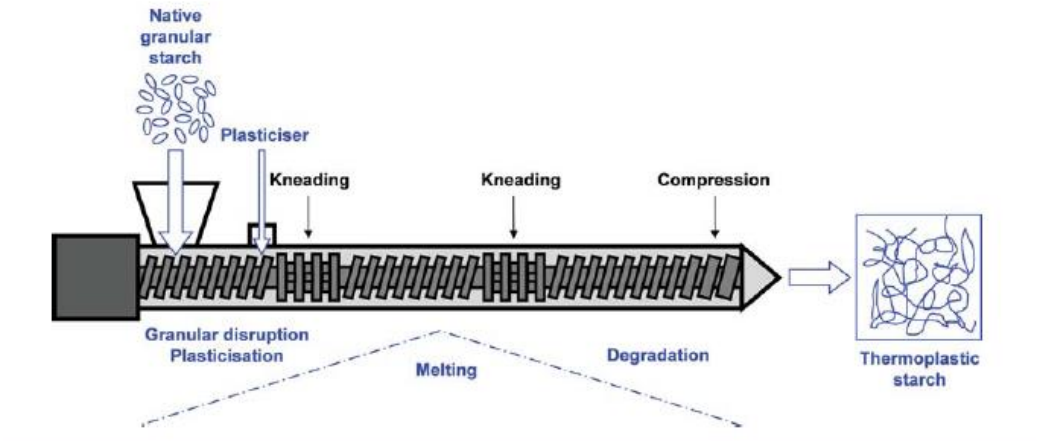

Figure 2.10. Twin-screw extruder schematic for thermoplastic starch production (Xie et al., 2012).

Starch is mixed with plasticizer, water, and other additives, the mixture is fed to extruder with a feeding unit. As the mixture travels through the barrel, it is subjected to heating, compression, and friction resulting in the formation of homogeneous molten compound (Thuwall et al., 2006). Plasticization of starch occurs in two steps. First, with the diffusion of plasticizer and starch granule partial fragmentation, viscosity of the

mixture increases. Second, with a complete fracture of the starch granules, a decrease in the viscosity of the mixture occurs. The fragmentation of the starch granules causes polymer material to become thermoplastic (Montilla-Buitrago et al., 2021). The main goal of thermoplastic starch extrusion is to complete melting and mixing without degradation, affecting the mechanical properties of the final product (Xie, Luckman, et al., 2014).

The main factors affecting extrusion process are moisture, composition of the mixture, plasticizer type and plasticizer concentration. Operational conditions, temperature, screw speed and pressure, are also important (Mehyar & Han, 2006). The amylose-to-amylopectin ratio changes with the starch source also affects the extrusion process depending on the mixture's viscosity. Temperature profile in the extruder is also an important parameter that depends on starch type. The range should be above the gelatinization temperature of the starch and below steam bubble formation which varies between 60-250^{o}C depending on the process (Singh & Genovese, 2021). High screw speed decreases the residence time; therefore, gelatinization of the starch could be reduced while increases the mixture mixing due to higher torque (Das, 2008). In TPS production, the starch mixture is generally conditioned by keeping it in weather-tight containers for 3 hours to 4 days before feeding to the extruder. This conditioning allows the plasticizer to diffuse into starch granules to ensure plasticization process (Arboleda et al., 2015).

In the study of Mitrus et al. (2009), extrusion of potato, corn and wheat starches was conducted to investigate the effect of glycerol content on glass transition temperature and mechanical properties of TPS. The moisture content was 15.5% for potato starch, 14.4% for corn starch and 14.2% for wheat starch. Potato starch has 24% amylose content whereas corn and wheat starches have 26% and 24%, respectively. Glycerol was used as plasticizer and added to starch with 15-30 wt.% by dry mass. The mixtures were prepared as 20 kg samples and stored in an air-tight bag for one day to facilitate glycerol penetration into starch granules. A single-screw extruder was combined with a high-speed cutter machine to form granules. Operating conditions for the extruder were 85-100°C barrel temperature with 80 rpm screw speed. With these extrusion conditions, TPS materials without steam bubbles were produced from potato starch. However, pores were observed for corn and wheat starches, similar to solid foams (Mitrus & Mooecicki, 2009).

The effect of glycerol content on glass transition temperature for TPS materials produced from potato, corn and wheat starches was shown in Fig. 2.11. Since a higher glass transition temperature causes brittleness, it is important to decrease the glass transition temperature of the TPS material. According to Fig. 2.11, increasing glycerol content decreased the T_g for all starches. The lowest glass transition was obtained in potato starch. For potato starch, the T_g of the TPS with 15% glycerol content were 132°C and it decreased to 18°C with 30% glycerol content. The amylose content of the starch type affected the glass transition temperature. Higher amylose content starches have lower T_g values for the same amount of glycerol suggesting that TPS produced from starches with higher amylose content are more flexible (Mitrus & Mooecicki, 2009).

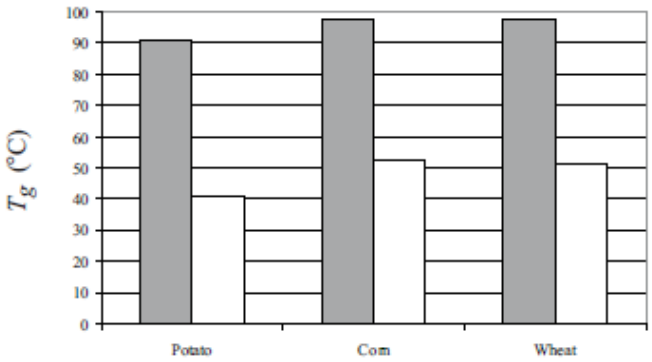

Figure 2.11. Glass transition temperature of potato, corn, and wheat TPS with ■ 20% glycerol and □ 25% glycerol contents (Mitrus & Mooecicki, 2009).

The mechanical properties of TPS materials were investigated with a compression test. The effect of glycerol content on tensile strength for potato, corn, and wheat starch TPS materials is shown in Fig. 2.12. The results showed low stress values for corn and wheat starches with 25% glycerol contents. The highest stress values were obtained from potato starch with 20% glycerol content. It was concluded that the mechanical properties of the TPS materials were not dependent only on amylose percent. It also depended on the starch's botanical source which varied in the molecular weight of the amylose (Mitrus & Mooecicki, 2009).

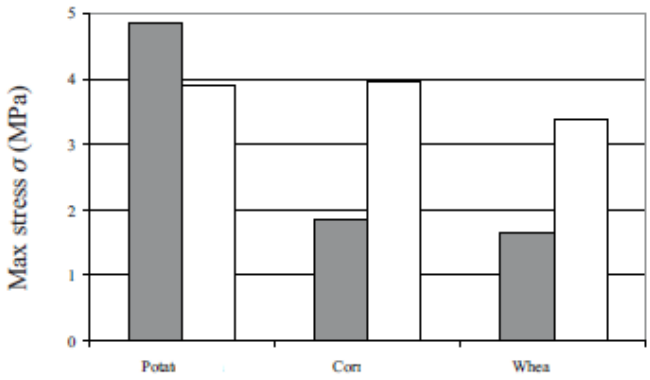

Figure 2.12. Tensile strength of potato, corn, and wheat TPS with ■ 20% glycerol and □ 25% glycerol contents (Mitrus & Mooecicki, 2009).

Extrusion of high amylose potato starch was considered as a more difficult process due to the high melting temperature of amylose resulting in high melting viscosity, unstable flow, and inadequate melting (Shogren, 1992). However, high amylose starch plastics have better strength and tough mechanical properties (Van Soest & Borger, 1997). Thuwall et al. studied (2006), the extrusion of normal potato starch and high-amylose potato starch. High amylose potato starch (HAP) had 86% amylose content, and normal potato starch (NPS) had 21% amylose content. Glycerol was added to 30 and 45 wt.% to starch by dry mass for both starches. For high amylose potato starch (HAP), different compositions were also studied by adding dextrin with 5 and 10 wt.% to decrease viscosity and by adding fluoro-elastomer lubricant with 3 wt.% to reduce sticking of the mixture to extruder die. Also, moisture content of the mixtures varied between 19 to 30 wt.%.

After compounding at 110^{o}C and 24 rpm the extrusion was conducted in a single screw extruder with 20 to 100 rpm. The obtained extrudates were pelletized by cutting into smaller pieces and conditioned at 50% and 70% relative humidity at 23^{o}C. The melt viscosity was measured, and not significantly affected by adding 3% fluoride elastomer lubricant to high amylose potato starch at a 45% glycerol ratio. However, the addition of 5% dextrin reduced the viscosity. The extrusion of HAP mixtures was more difficult compared to NPS due to melt's higher viscosity. The upper moisture contents of the mixtures were determined as 17 wt.% for NPS and 30 wt.% for HAP to prevent bubble formation at 160^{o}C. The extrusion was successful at 160^{o}C for HAP with 100:45 glycerol content and 30% moisture content.

The mechanical properties of the extrudates with 45 wt.% glycerol content after conditioning at 23ºC and 53% relative humidity were shown in Table 2.2. The tensile strength was approximately 40 MPa for both HAP and NPS. However, adding 5% dextrin increased HAP's tensile strength to 68 MPa. The high melt viscosity of HAP material was attributed to more complicated amylose structure, which results in higher tensile strength values. Overall, better mechanical properties were obtained for high amylose starch mixtures.

Table 2.2. The mechanical properties of extrudates with different compositions (Thuwall et al., 2006b).

	Tensile Modulus (MPa)	**Strain at Break (%)**	**Stress at Break (MPa)**
NPS 100:45	45	47	3
HAP 100:45	36	80	4.9
HAP 100:45 + 5% dextrin	68	67	5

In the study of González-Seligra et al. (2017), the effect of extrusion screw speed on starch film morphology was examined. A 100 g extruded blend was prepared by mixing cassava starch, glycerol, and water to a 3:1:1 weight ratio. The extrusion temperature profiles were ranged between 90-140ºC, and screw speeds were selected as 40, 80 and 120 rpm in a twin-screw extruder. The extruded samples were transformed to pellets by cutting and then the obtained pellets were pressed into film forms at 140ºC and 120 rpm for 15 minutes. The films were conditioned at 56% relative humidity before testing.

The morphology of the thermoplastic materials before pelletizing was analyzed by field emission SEM (FE-SEM). In Fig. 2.13., the SEM images were shown for obtained thermoplastic starches where T40, T80 and T120 stand for screw speeds of 40, 80 and 120 rpm. A homogeneous and smooth surface was obtained for T80 material suggesting enough processing for product formation. However, both T40 and T120 starch grains were obtained and circulated in Fig. 2.13. The presence of starch grains suggested an incomplete gelatinization process, which prevented the breaking of all starch granules. Therefore, 40 rpm screw speed was considered insufficient for the extrusion process. Also, when the extrusion rpm increases, the specific mechanical energy increases. If the

specific mechanical energy was sufficient for thermoplastic starch extrusion process, a homogeneous surface structure was expected, breaking all starch granules. Even though T120 thermoplastic starch was processed with more energy consumption compared to T80, unbroken starch granules were observed in the material. This was attributed to the less time the mixture spent in the extruder with higher rpm. The optimum rpm was selected as 80 rpm for the full gelatinization process.

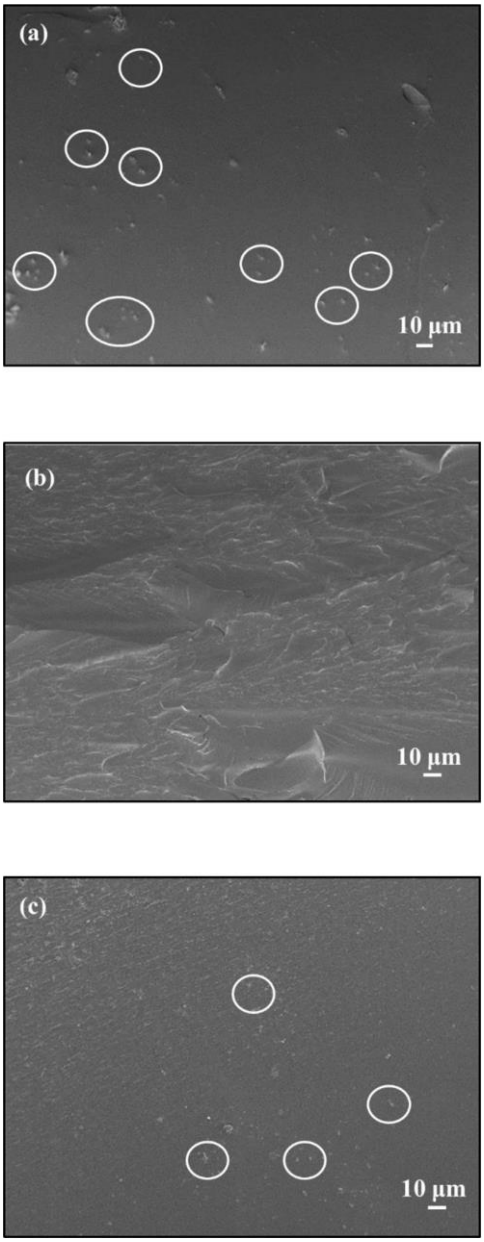

Figure 2.13. FE-SEM images of extruded starches at 40 rpm (a), 80 rpm (b) and 120 rpm (c) (González-Seligra et al., 2017).

The obtained films were also analyzed with SEM to compare the morphology. The SEM images in Fig. 2.14. shows the starch grains for TPS40; however, for TPS120,

the observed starch grains disappeared after the pressing process which could be related to complete gelatinization or melting of the granules with temperature and pressure. Therefore, extrusion at 120 rpm combined with pressing was considered suitable for homogeneous film production.

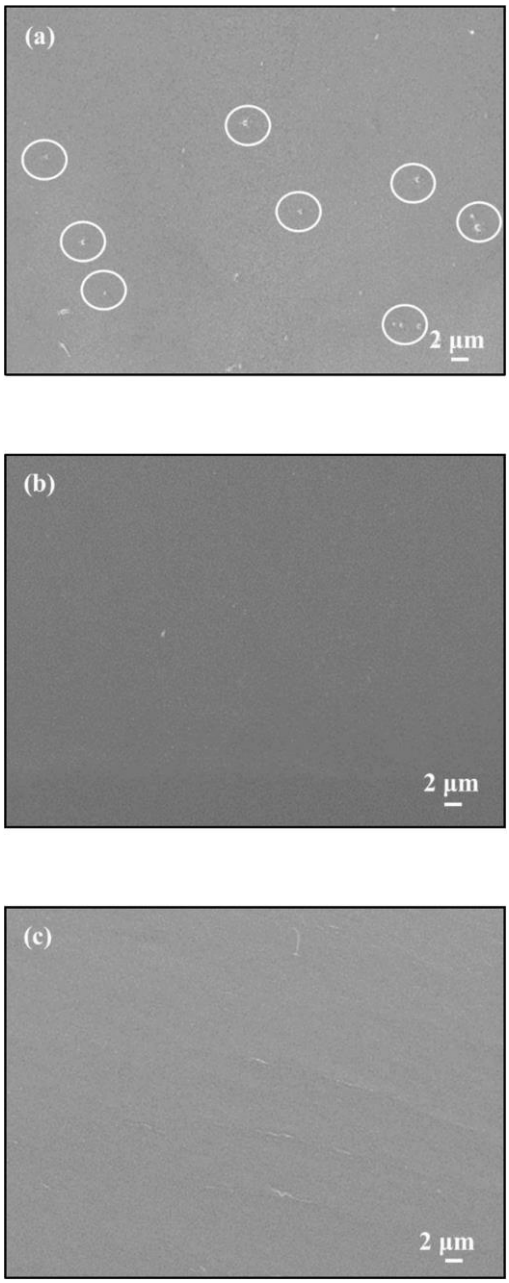

Figure 2.14. FE-SEM images of pressed starch films extruded at 40 rpm (a), 80 rpm (b) and 120 rpm (c) (González-Seligra et al., 2017).

The mechanical properties were measured as tensile strength, Young's modulus, and strain at break and shown in Table 2.3. According to obtained mechanical properties,

TPS40 and TPS120 showed better tensile strength and Young's modulus value than TPS80. However, the highest strain at break value was observed for TPS80. This was attributed to starch grains in TPS40 and TPS120 materials, which were good at fissure propagation. To conclude, conducting extrusion at 80 rpm produced desirable homogeneous products; however, operating at 120 rpm resulted in better mechanical properties.

Table 2.3. The mechanical properties of the obtained extrudates (González-Seligra et al., 2017).

	Tensile Strength (MPa)	**Young's Modulus (MPa)**	**Strain at Break (%)**
TPS40	1 ± 0.2	21 ± 2	45 ± 5
TPS80	0.55 ± 0.08	9 ± 1	78 ± 5
TPS120	1.4 ± 0.2	21 ± 2	65 ± 5

2.6. Specific Mechanical Energy

Specific mechanical energy (SME) is defined as the amount of motor power that is being input for processing each kg of material. SME is formulated as Equation (2.1) (Janssen et al., 2002; Levine, 1997);

$$\mathrm{SME} = \frac{n * P * O}{n_m * Q} \qquad (2.1)$$

where, n is screw rotations (1/min); n_m is maximal screw rotations (1/min); P is rated power (kW); O is engine loading (%); and Q is extruder capacity (kg/h). In Table 2.4., the specific mechanical energy consumptions required for processing different starches by extrusion under different extrusion conditions were shown.

Table 2.4. The mechanical properties of the obtained extrudates (González-Seligra et al., 2017).

Starch Type	Extrusion Conditions	Specific Mechanical Energy (SME)	Reference
Wheat, maize and rice starch	- Twin screw extruder - Temperature: 90 – 150°C - Screw speed: 190 – 390 rpm	0.081–0.365 $kWhkg^{-1}$	(Bindzus et al., 2002)
Maize starch	- Twin screw extruder - Temperature: 70 – 190°C - Screw speed: 200 – 400 rpm	0.1 to 0.25 $kWhkg^{-1}$	(Brümmer et al., 2002)
Potato starch	- Twin screw extruder - Temperature: 120 – 210°C - Screw speed: 140 – 200 rpm	0.1 to 0.32 $kWhkg^{-1}$	(Valle et al., 1995)

In the study of Combrzyński et al. (2012), extrusion of potato and cereal starches were conducted in a single screw extruder. Specific mechanical energy consumption and process efficiencies were investigated by varying starch types, glycerol contents and extrusion screw speed. Starch types were potato, corn, and wheat. Glycerol contents ranged between 15-30 wt.% by starch dry mass. The extrusions were conducted between 80 to 100°C with 80 and 100 rpm values. A standard register was connected to the motor to measure power consumption for each of the mixture composition and screw speeds.

Fig. 2.15. shows the process efficiency in terms of the amount of extrudate produced in an hour for different starch types and glycerol contents. The efficiency was higher for potato starch and decreased with increasing glycerol content. The main difference in process efficiency for different starch types was attributed to amylose content, which affects the mixture viscosity and processing in the extruder. Also, in multi-extrusion, efficiency decreased with increasing extrusion times regardless of the glycerol content, as shown in Fig. 2.16.

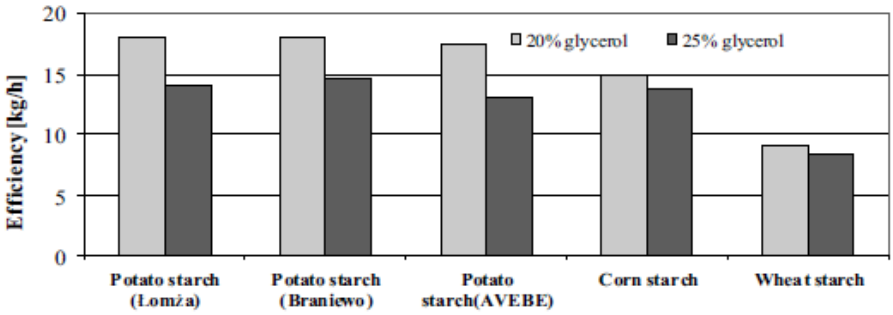

Figure 2.15. Process efficiency of the extrusion with various starch types and glycerol content (Combrzyński et al., 2012).

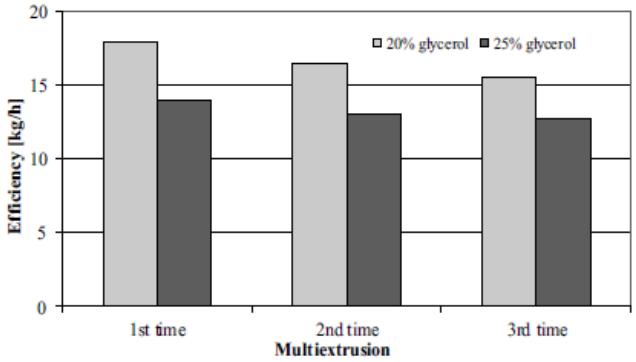

Figure 2.16. Process efficiency of multi-extrusion with varying glycerol content (Combrzyński et al., 2012).

The specific mechanical energy is an important criterion to determine the unit cost of the product. Fig. 2.17. shows that the lowest specific mechanical energy was obtained for Braniewo potato starch with 25% glycerol content among different starch types and glycerol contents. According to the results in Fig. 2.18., SME decreased with increasing glycerol content and increased with increasing screw speed. The average SME was around 0.07 kWh.kg-1, and the minimum SME was observed for the mixture with 30% glycerol content processed at 80 rpm. The SME value for 15% glycerol content was 0.060 kWh.kg-1 at 80 rpm and 0.068 kWh.kg-1 at 100 rpm.

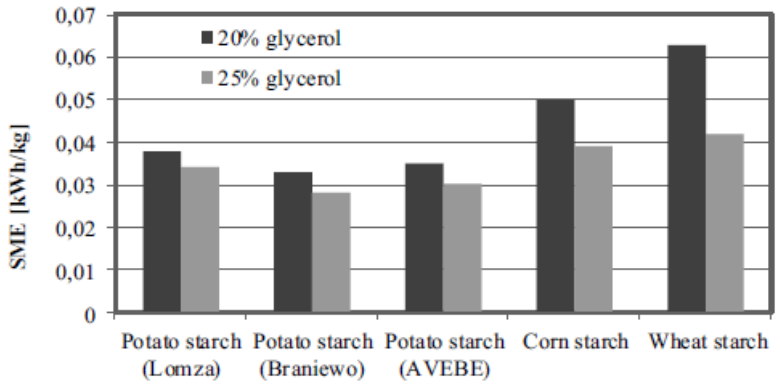

Figure 2.17. Specific mechanical energy consumption for different starch types with varying glycerol content (Combrzyński et al., 2012).

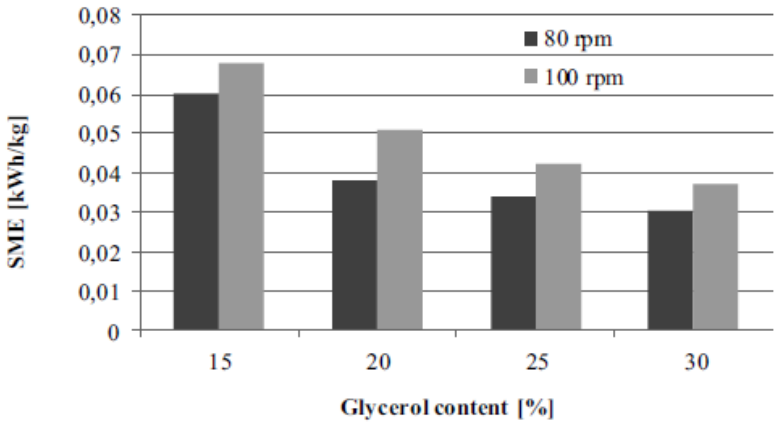

Figure 2.18. Specific mechanical energy consumption for different rpm values with varying glycerol content (Combrzyński et al., 2012).

In the study of Oniszczuk et al. (2015), the effect of flax fibers addition and screw rotation on extrusion of thermoplastic corn starch was examined. Flax fiber with 10, 20, and 30 wt.% was mixed with corn starch containing 20 wt.% glycerol as a plasticizer. Before extrusion, the prepared mixtures were stored in a plastic bag for one day to enhance glycerol penetration into starch granules. The extrusion was conducted in a single screw extruder with a 3 mm die diameter and a cooling system. Extrusion temperatures were set between 60 to 110°C and screw speed were selected as 60, 80 and 100 rpm. The specific mechanical energy consumption was measured by determining process efficiency and motor load. The radial expansion index, the ratio of pellet diameter to die diameter, was also calculated.

Fig. 2.19. shows the effect of flax fibers content and screw rpm on process efficiency. The efficiency increased by increasing the screw speed but decreased with the increased flax fiber content due to the length of flax fibers resulting in lower mixing. The highest efficiency was obtained as 27.6 $kg.h^{-1}$ for mixture with no flax fiber content extruded at 100 rpm and the lowest efficiency was obtained as 11.04 kg/h^{-1} with 30% flax fiber content extruded at 60 rpm.

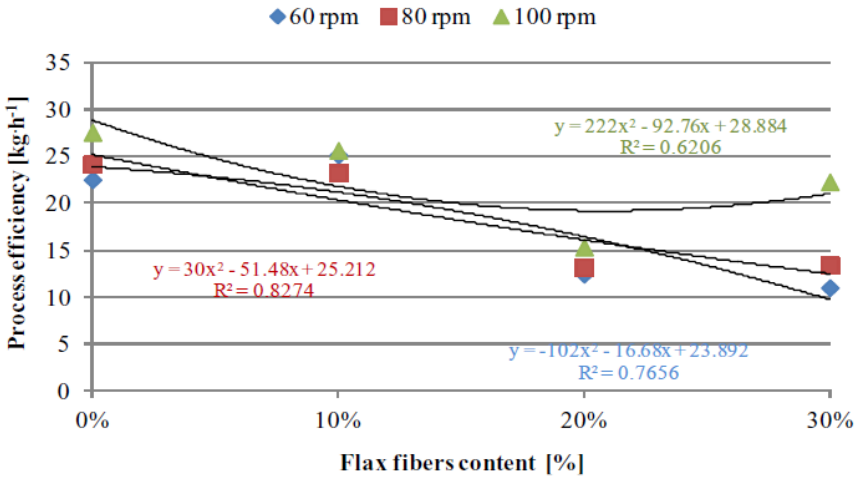

Figure 2.19. Effect of flax fiber content and screw rpm on process efficiency (Oniszczuk et al., 2015).

Fig. 2.20. shows the effect of both flax fibers content and screw rpm on the specific mechanical energy consumption. Although the specific mechanical energy consumption increased with the increased speed and flax fiber content, the effect of screw speed was more dominant. The screw speed affects the energy consumption directly with more torque demand. The increase in specific mechanical energy consumption with flax fiber content was related to the presence of long-length fibers, which creates more resistance in the extrusion process. The highest SME consumption was 0.226 $kWh.kg^{-1}$ for 30% flax fiber content extruded at 100 rpm and the lowest SME consumption was obtained as 0.056 $kWh.kg^{-1}$ for no flax fiber addition extruded at 60 rpm.

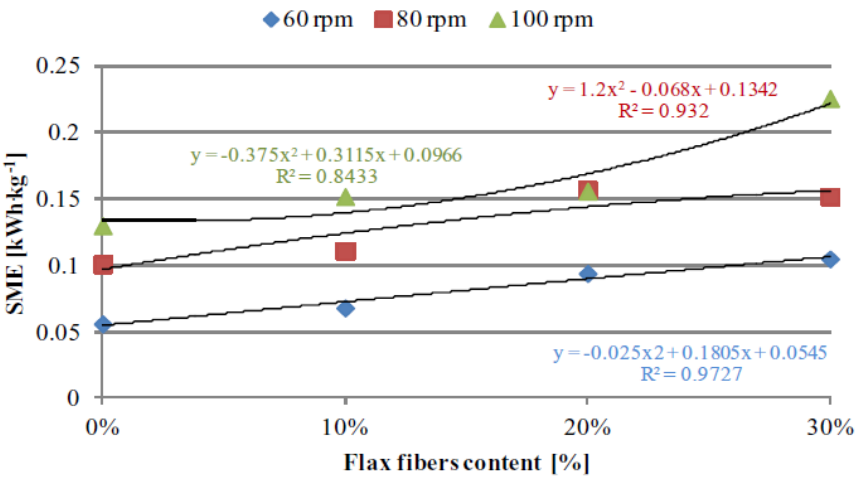

Figure 2.20. Effect of flax fiber content and screw rpm on specific mechanical energy consumption (Oniszczuk et al., 2015).

The influences of flax fiber content and screw rpm on radial expansion index were shown in Fig. 2.21. The radial expansion index decreased with increasing flax fiber content and increased with the screw speed. The highest values were obtained with no addition of flax fiber content. The obtained values were considered typical for extruded plant material.

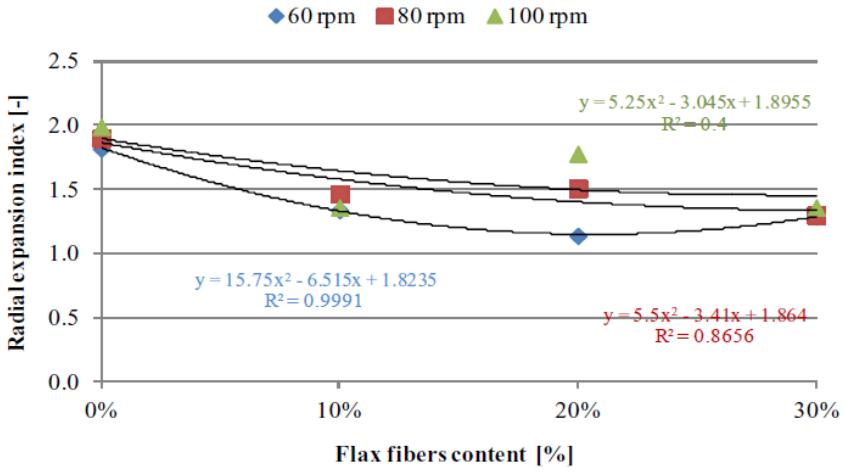

Figure 2.21. Effect of flax fiber content and screw rpm on radial expansion index (Oniszczuk et al., 2015).

In the study of Combrzyński et al. (2020), the production of potato starch-based foams by extrusion was investigated. The foams were produced with polyvinyl alcohol as foaming agent. The effect of polyvinyl alcohol (PVA) amount, type of die, moisture

content of the mixture and screw speed on the process efficiency and specific mechanical energy consumption were studied. The mixtures were prepared by adding polyvinyl alcohol to potato starch with 1, 2 and 3 wt.%. Then the moisture of the mixtures was adjusted to 17, 18 and 19 wt.% by adding water. The extrusion was conducted in a single-screw extruder below 120°C. Screw speeds were selected as 100 and 130 rpm. Also, two types of dies were studied as circular and ring with 3- and 5-mm diameters respectively.

The extrusion process efficiencies with different combinations of screw speed and die type at different moisture level and PVA additive amount were shown in Fig. 2.22. In the figure, die types were represented as M1 for circular die and M2 for ring die; screw speeds were represented as S1 for 100 rpm and S2 for 130 rpm and addition of polyvinyl alcohol was represented as A1 for 1%, A2 for 2% and A3 for 3%. The process efficiency values were obtained between 25 – 44 kg/h. The efficiency was increased with increasing moisture content, PVA amount, screw speed, and by using circular type dies. The highest efficiency observed was 44 kg/h for 3% PVA addition at 19% moisture content extruded at 130 rpm with circular die.

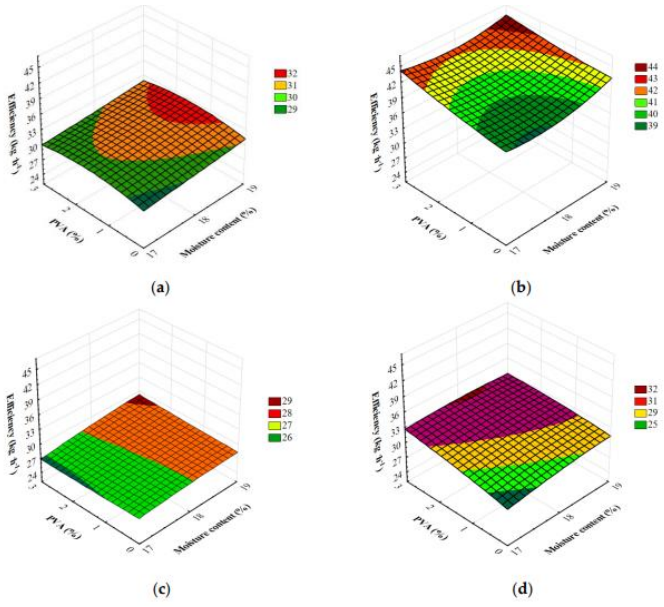

Figure 2.22. The extrusion efficiency of starch-based foams at different process conditions represented by (a) M1-S1 (b) M1-S2 (c) M2-S1 (d) M2-S2 (Combrzyński et al., 2020).

The specific mechanical energy consumption at different processing conditions varied between 0.070 - 0.121 kWh/kg, as shown in Fig. 2.23. According to results, processing at higher screw rotation or with the ring die type consumed more energy than

the circular die type. Energy consumption was lower to process the mixture with higher moisture content due to the plasticizing effect of water. On the other hand, increasing the additive content resulted in higher energy consumption attributed to processing more polymeric material.

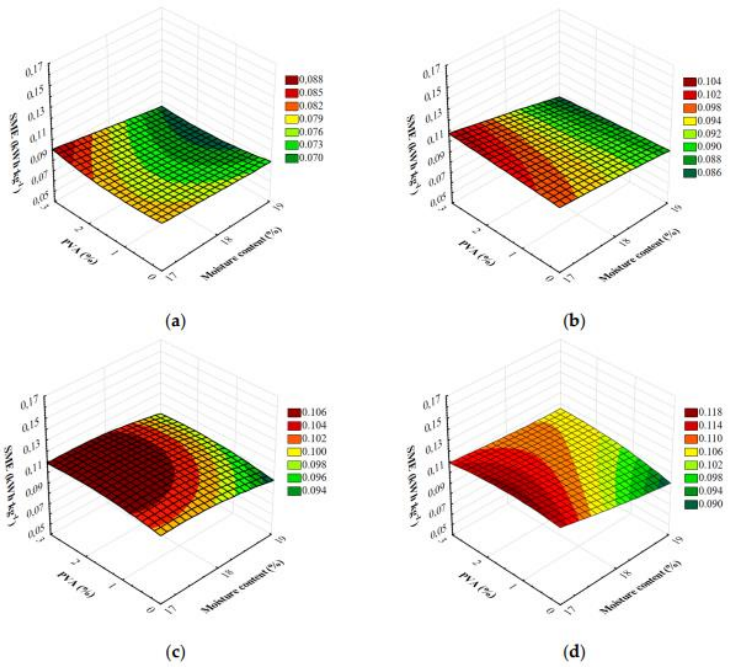

Figure 2.23. The specific mechanical energy consumption at different process conditions represented by (a) M1-S1 (b) M1-S2 (c) M2-S1 (d) M2-S2 (Combrzyński et al., 2020).

Compression tests were conducted to investigate the produced material's useful properties, and the results are shown in Fig. 2.24. The resistance for compression values corresponding to the material's stiffness varied between 133 - 935 MPa. According to the results, higher stiffness of the materials was observed with circular die, 130 rpm screw rotation and increased PVA amount and moisture content. The obtained resistance for compression values was similar in the range of commercial foams.

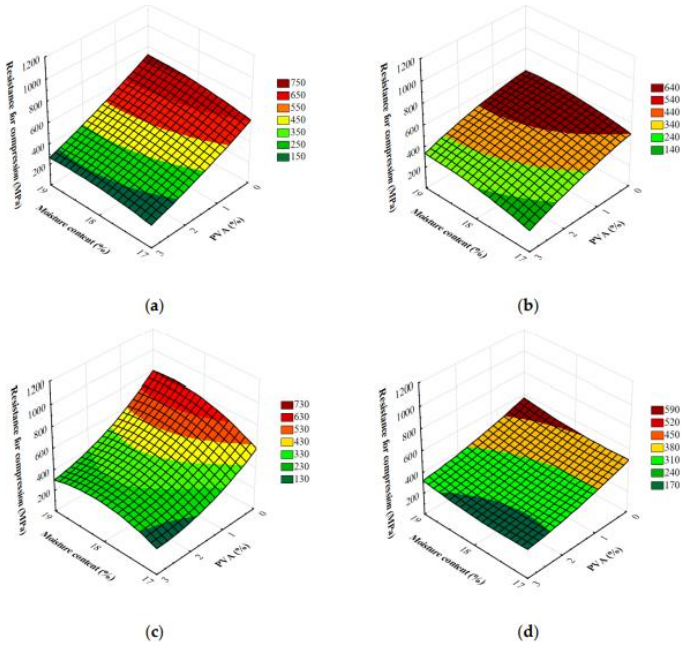

Figure 2.24. The resistance for compression values at different process conditions represented by (a) M1-S1 (b) M1-S2 (c) M2-S1 (d) M2-S2 (Combrzyński et al., 2020).

CHAPTER 3

EXPERIMENTAL

3.1. Materials

The source of the residual potato starch was the production lines of potato chips from the PepsiCo company. While the potato was washed and cut into slices, the potato starch was obtained by filtering the flowing water with a decanter. The potato starch was dried and sieved by the Ilginlar Industrial Food Recovery and Feed Raw Materials Logistics Industry Trade Inc. Vegetable based glycerol (99.7% purity) was obtained from Alfasol.

3.2. Methods

3.2.1. Pretreatment of the Raw Material

The raw material arrived at Ilgınlar Industrial Food Waste Recovery company as residual potato starch with 40 wt.% moisture content and containing impurities. The company pretreated the initial residual starch by sieving with 131μm mesh size and drying to 10 wt.% moisture content. The pretreated starch was stored in plastic bags, as shown in Fig. 3.1. Extrusion trials were conducted with pretreated potato starch.

Figure 3.1. Pretreated potato starch stored in plastic bags.

3.2.2. Moisture Content Determination

The potato starch's moisture content was determined according to the "ISO 6496 Determination of Moisture and Other Volatile Matter Content for Animal Feeding Stuff" procedure. A glass container and lid were dried in an electrically heated oven at 103ºC for 30 minutes. Then, they were cooled to room temperature in a desiccator and weighed. The starch sample was spread into the container as 5 grams and dried in the oven at 103ºC for 4 hours with a lid beside it. After 4 hours, the sample was cooled to ambient temperature in a desiccator and weighted. The moisture content was calculated with Equation (3.1);

$$w_1 = \frac{m_1 - (m_3 - m_2)}{m_1} \, x \, 100\% \qquad (3.1)$$

where m_1 is the mass of the test portion; m_2 is the mass of the container with lid; and m_3 is the mass of the dried test portion including container and lid.

3.2.3. Mixture Preparation

The mixture of starch and glycerol was prepared in a plastic vessel for 2.5 kg for each extrusion trial. To prepare mixture with 20, 30 and 40 wt.% glycerol; 396.8-, 595.2- and 793.7-ml glycerol were added to 2.5 kg of potato starch, respectively. After adding glycerol, the mixture was mixed with an electric mixer for two minutes. The plastic container lid was closed, and the mixture waited three hours before the extrusion. Then, the mixture was sieved with a regular sieve to obtain a homogeneous form and prevent flocculation before feeding to extruder.

3.2.4. Extrusion Process

The extrusion was conducted in a single screw extruder. In Fig. 3.2., the single screw extruder, which has an external feeder and four temperature units, was shown. The extruder was connected to a three-phase electric motor. The electric motor type was

Gamak AGM2E132S4a and the technical values of the motor were 5.5 kW rated output power, 11.20 A rated current, 1430 rpm rated speed and 0.81 cosφ power factor. The temperature controllers with ± 1°C precision were connected to extruder units.

Figure 3.2. Single-screw extruder.

The extrusion temperatures were selected between the potato starch's gelatinization temperature and the water's boiling point. The formation of steam bubbles was attributed to the moisture content of the starch. Products with steam bubbles were not considered applicable in industrial production. Gelatinization temperature starts from 45°C for potato starch, and the steam bubble formation was observed for temperature values higher than 90°C (Lizarazo H. et al., 2015). Therefore, three different temperature sets alongside the extruder units were selected between 50-90°C, 60-90°C, and 70-90°C, as shown in Table 3.1. The unsteady-state period of the extrusion causes the die temperature to increase; therefore, the extruder die temperature was set for 90°C for all the experiments. Since there was no additional cooling system to decrease the temperature, it was set as 90°C from the beginning of the experiments.

Table 3.1. Temperature profiles in the extruder for four different temperature units.

Temperature Profile	Temperature Range
1st Set	50°C - 90°C
2nd Set	60°C - 90°C
3rd Set	70°C - 90°C

Extrusion trials were conducted for 20, 30 and 40 wt.% glycerol mixtures by using pretreated starch which has 10% moisture content and sieved with 131μm mesh size. In Table 3.2, these product's labels were shown by indicating moisture content, mesh size, glycerol amounts and extrusion temperature profiles.

Table 3.2. Product labels which indicate glycerol amount and temperature profile.

Product	Moisture Content	Mesh Size	Glycerol Amount	Temperature Profile
TPS201	10%	131μm	20 wt.%	1st Set
TPS202	10%	131μm	20 wt.%	2nd Set
TPS203	10%	131μm	20 wt.%	3rd Set
TPS301	10%	131μm	30 wt.%	1st Set
TPS302	10%	131μm	30 wt.%	2nd Set
TPS303	10%	131μm	30 wt.%	3rd Set
TPS401	10%	131μm	40 wt.%	1st Set
TPS402	10%	131μm	40 wt.%	2nd Set
TPS403	10%	131μm	40 wt.%	3rd Set

Additional pretreatment conditions were also studied to examine the effect of pretreatment on specific mechanical energy consumption and mechanical properties of the produced TPS. One more different mesh-sized sieve was used, and another additional moisture content for the starch was selected. To examine the effect of sieving, the residual potato starch was sieved with 300μm mesh size, initially dried to 10 wt.% moisture content. Also, to investigate the effect of moisture content, the residual potato starch was dried to 26 wt.% moisture content which was sieved initially with 131μm mesh size.

These two additional starches were extruded with the first temperature set and 30 wt.% glycerol amounts. These samples were labeled as shown in Table 3.3.

Table 3.3. Product labels which indicate glycerol amount and temperature profile for differently pretreated starch.

Product	Moisture Content	Mesh Size	Glycerol Amount	Temperature Profile
TPSS1	10%	300μm	30 wt.%	1st Set
TPSM1	26%	131μm	30 wt.%	1st Set

For the cleaning of the extruder, zinc stearate was used. Zinc stearate is a commonly used lubricant in extrusion processes for the plastic industry. As an extruder lubricant, it is used as solid additive to improve product homogeneity, prevent hot spot formation and decrease energy consumption (Adplast, 2023). However, it was only used for cleaning purposes in the experiments. After each extrusion trial, 50 g of zinc stearate were passed through the extruder for preventing the residual starch mixtures to stick to the screw of the extruder.

3.2.5. Specific Mechanical Energy Consumption

To calculate the specific mechanical energy consumption, the motor load was obtained from the driver of the electric motor. For the Atv310 motor driver, the 810-monitoring mode was selected showing the output power percentage. The output power represents the ratio between estimated motor power (on the shaft) versus drive rating. Also, the capacity of the extruder was measured by collecting the extrudate for 30 seconds and weighing the sample. The rpm of the motor was always at full capacity, selected as 100% rpm shaft in the extruder.

3.2.6. Particle Size Distribution Analysis

The particle size distribution of two different starches were analyzed by Dynamic Light Scattering Zeta Sizer. The starch, sieved with 131μm mesh size, weighed 0.0136 g,

and the starch, sieved with 300µm mesh, weighed 0.0139 g, was mixed with distilled water in a 2 ml holder using a vortex mixer. The measurement conditions were set as 25^{o}C temperature, 0.8878 cP viscosity, 11928 cps intensity and 1.3272 refractive index. The analysis was repeated three times for each starch sample to obtain an average value.

3.2.7. Mechanical Testing

The mechanical tests were conducted according to the "ASTM D638 Standard Test Method for Tensile Properties of Plastics" procedure using the Testometric materials testing machine (Model No X350). First, the extrudates were molded into dog bone shapes. The dimensions of the dog bone shape were selected from the ASTM D638 procedure as Type IV which was used for samples smaller than 4 mm in thickness. In Fig. 3.3., the shape of the Type IV samples was shown, and the dimensions are given in Table 3.4.

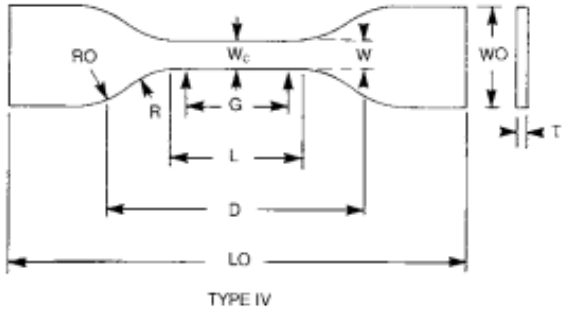

Figure 3.3. Illustration of the Type IV specimen.

Table 3.4. Specimen dimensions for dog bone shape of Type IV.

Dimensions	Type IV (mm)
W-Width of narrow section	6
L-Length of narrow section	33
WO-Width overall	19
LO-Length overall	115
G-Gage Length	25
D-Distance between grips	65
R-Radius of fillet	14
RO-Outer radius	25

The conditioning of the samples was conducted at 25ºC and 50% relative humidity for 24 hours according to standard before mechanical testing. For each of the TPS material, five specimens were tested to obtain average value with standard deviation. The test speed was 5 mm/min for 40 mm sample length. Tensile strength, elongation at break and Young's modulus values were obtained by the analysis of the mechanical testing results. The stress is defined as the force per unit area and calculated with Equation (3.2).

$$\sigma = \frac{F}{A} \qquad (3.2)$$

where F is the force and A is the cross-sectional area of the sample.

The strain is defined as the extension per unit length and calculated with Equation (3.3).

$$\varepsilon = \frac{L - L_0}{L_0} \qquad (3.3)$$

where L is the length of the sample after stretching and L_0 is the original length of the sample being stretched. The tensile strength at break was calculated with Equation (3.2) with the force at peak value. The Young's modulus was calculated with Equation (3.4).

$$E = \frac{\sigma}{\varepsilon} \qquad (3.4)$$

where σ is the stress and ε is the strain. The elongation at break was calculated by Equation (3.5).

$$e = \frac{L - L_0}{L_0}\, x\, 100 \qquad (3.5)$$

CHAPTER 4

RESULTS AND DISCUSSION

4.1. Particle Size Distribution

Fig. 4.1. and 4.2. show the particle size distributions for two types of starches, which were sieved with 131µm and 300µm mesh size, respectively. The average particle sizes were found to be 103.44µm and 108.43µm for the starch samples, sieved with 131µm and 300µm mesh sizes. Although the samples' average sizes were similar, during storage, microbial activity was observed for the residual potato starch sieved with a 300µm mesh size as a result of the contaminants not separated from the starch with higher than 131µm particle size. Therefore, a 131µm mesh-sized sieve was selected for the pretreatment of the residual potato starch.

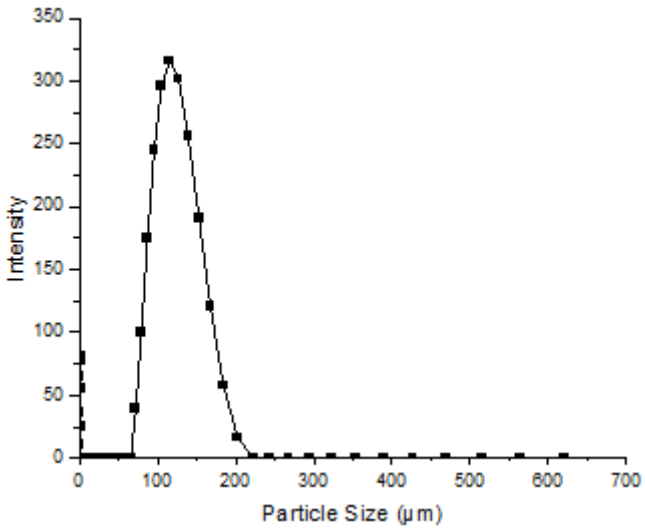

Figure 4.1. Particle size distribution for 131µm mesh size sieved residual starch.

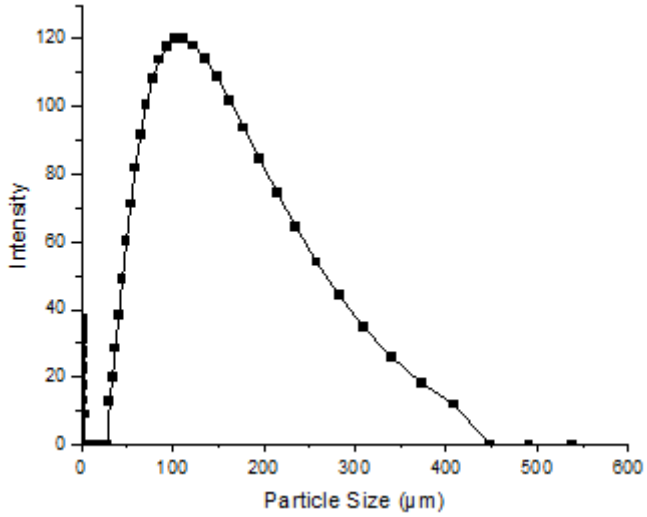

Figure 4.2. Particle size distribution for 300µm mesh size sieved residual starch.

4.2. Specific Mechanical Energy Consumption

The successful extrusion process requires continuous production of extrudates without causing steam bubbles generation. However, these requirements were not satisfied for the samples coded as TPS202 and TPS203, as the extrudates had steam bubbles, and continuous production was impossible. As a result, no mechanical testing was conducted for the TPS202 and TPS203 since dog bone-shaped samples were not obtained. The specific mechanical energy consumption values for the successfully produced extrudates are shown in Table 4.1.

Table 4.1. Specific mechanical energy values for the products.

Product	SME ($kWhkg^{-1}$)
TPS201	31.51
TPS202	8.96
TPS203	8.58
TPS301	43.27
TPS302	24.19
TPS303	23.78
TPS401	22.26
TPS402	11.30
TPS403	7.89
TPSS1	22.92
TPSM1	18.30

The SME values were in the range of 8.96-43.27 $kWhkg^{-1}$, which were higher than the value of 0.07 $kWh.kg^{-1}$ reported for potato starch extruded in a single-screw extruder (Combrzyński et al., 2012). The difference in energy consumption can be attributed to the origin of the potato starch, different screw configuration, and extrusion temperature. The highest SME value was obtained for the TPS301 (43.27 $kWhkg^{-1}$) and the lowest for the TPS403 (7.89 $kWhkg^{-1}$) coded samples. Although calculated, it is not possible to compare relatively lower energy consumptions obtained for TPS202 and TPS203 with the SME values of other extrudates due to difficulties in the extrusion of these samples and steam bubble formation.

4.2.1. Effect of Pretreatment on Specific Mechanical Energy Consumption

4.2.1.1. Effect of Moisture Content on Specific Mechanical Energy Consumption

The effect of moisture content on the properties of extrudates was investigated by processing 10 wt.% and 26 wt.% moisture content starches. The glycerol content in the

samples was 30 wt.%, and the temperature range during extrusion was 50-90°C. The extrudates, labeled as TPS301 and TPSM1, had SME values of 43.27 $kWhkg^{-1}$ and 18.30 $kWhkg^{-1}$, respectively. Combrzyński et al. (2012) reported increased SME values with the increased moisture content, while Su et al. (2009) reported the opposite result, per our results. The decrease in SME values with higher moisture content was attributed to the plasticizer effect of water and the lower torque needed for extrusion. Starch mixture with a high moisture content easily stuck to the extruder die, which required further cleaning after extrusion.

4.2.1.2. Effect of Sieving on Specific Mechanical Energy Consumption

Starch samples, sieved with 131μm (sample code TPS301) and 300μm mesh (sample code TPSS1), containing 30 wt.% glycerol, were extruded at 50-90°C temperature intervals. The SME values were 43.27 $kWhkg^{-1}$ and 22.92 $kWhkg^{-1}$ for TPS301 and TPSS1, respectively. Even though there was no remarkable difference in average particle size, the energy consumption decreased with the increased particle size. The decrease in energy consumption with increasing average particle size was also reported by Carvalho et al. (2010). Large particles are less impacted by barrel temperature than finer particles because they have a smaller surface area of interaction with other particles and with the barrel. Therefore, the melt transition temperature would be reached by the finer particles more quickly than the coarser particles, resulting in reduced viscosity and lower specific mechanical energy consumption. However, mold formation occurred in the residual starch sieved with a 300μm mesh size, making this pretreatment not an applicable option for long-term storage.

4.2.2. Effect of Glycerol Content on Specific Mechanical Energy Consumption

Fig. 4.3. shows the effect of glycerol content on the SME consumption for the TPS production. The SME values were highest for 30 wt.% glycerol content with an average of 30.42 $kWhkg^{-1}$ and lowest for 40 wt.% glycerol content with an average of

13.82 kWhkg^{-1}. Higher SME values were for the samples with 30 wt.% glycerol content for all the temperature sets than 40 wt.% glycerol. Mitrus et al. (2005) also reported decreased SME values with increasing glycerol content. The potato starch glycerol mixture displays a non-Newtonian fluid behavior in which viscosity decreases non-linearly as a function of shear rate. The increase in the glycerol content has a diluting effect on the mixture. Adding more glycerol results in more interaction as hydrogen bonds between starch and glycerol, which decreases the mixture's viscosity (Ayala et al., 2014). Therefore, increasing glycerol content in the mixture results in lower energy demand for processing. The unexpectedly low SME values obtained with 20 wt.% glycerol content was attributed to processing problems and steam bubble formation.

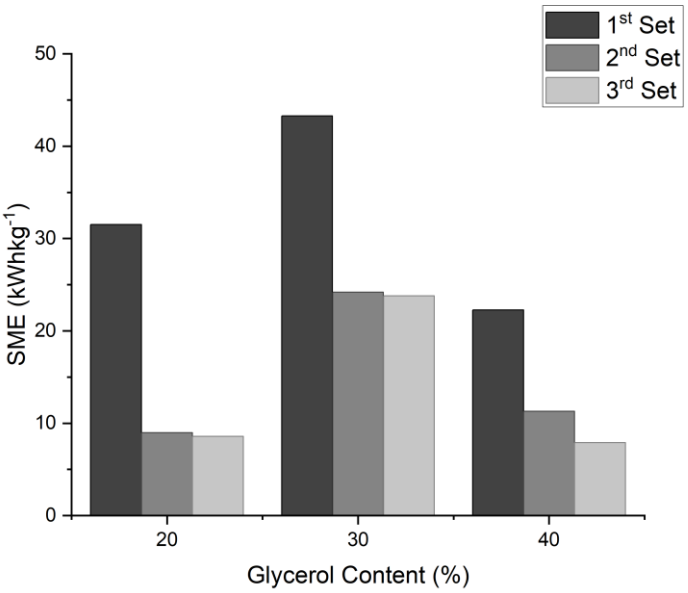

Figure 4.3. The effect of glycerol content on specific mechanical energy for different temperature sets.

4.2.3. Effect of Temperature on Specific Mechanical Energy Consumption

Fig. 4.4. shows the effect of the initial zone temperature on the SME consumption for producing the TPS with different glycerol content. Increasing the initial zone temperature from 50 to 60^{o}C reduced the SME consumption for all glycerol contents, but

the reduction was insignificant with a further increment from 60 to 70°C. The lowest SME values obtained with the initial zone temperature of 70°C were 8.58 $kWhkg^{-1}$ for TPS203, 23.78 $kWhkg^{-1}$ for TPS303, and 7.89 $kWhkg^{-1}$ for TPS403. Increasing the initial zone temperature causes more breakdown in the polymer structure and disruption of inner hydrogen bonds, thus decreasing the solution viscosity (Ayala et al., 2014), which results in lower SME values.

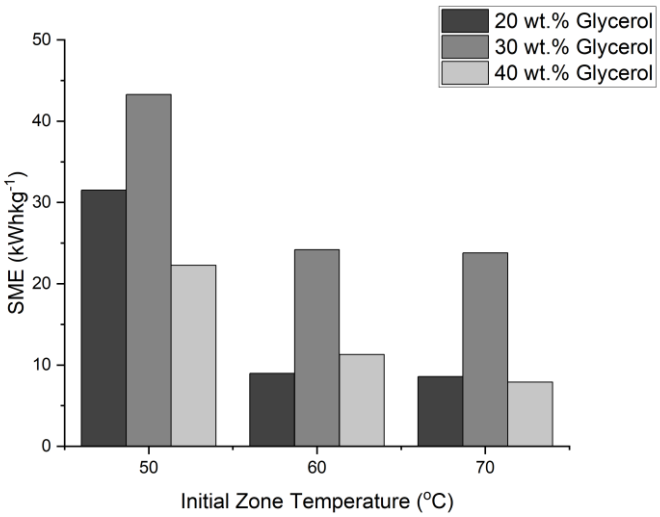

Figure 4.4. The effect of temperature sets on specific mechanical energy for different glycerol contents.

4.3. Mechanical Properties of the Extrudates

Fig. 4.5. shows the images of extrudates with 20 wt.% glycerol content extruded at different initial temperatures, 1st, 2nd and 3rd temperature sets, respectively. The steam bubble formation was observed for the 2nd and 3rd temperature sets as shown in the figure.

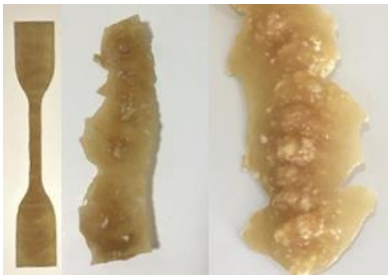

Figure 4.5. Extrudates with 20 wt.% glycerol content.

Fig. 4.6. shows the images of extrudates with 30 wt.% glycerol content extruded at different initial temperatures, 1st, 2nd and 3rd temperature sets, respectively.

Figure 4.6. Extrudates with 30 wt.% glycerol content.

Fig. 4.7. shows the images of extrudates with 40 wt.% glycerol content extruded at different initial temperatures, 1st, 2nd and 3rd temperature sets, respectively.

Figure 4.7. Extrudates with 40 wt.% glycerol content.

Fig. 4.8. shows the images of TPSS1 and TPSM1. TPSS1 was obtained with slightly greener color because of the microbial activity initially observed on the starch.

Figure 4.8. TPSS1 and TPSM1.

Table 4.2 lists the average mechanical properties of each of the five specimens and the standard deviations. No mechanical testing was conducted for the TPS202 and

TPS203 since they were not in the proper form. The higher standard deviation for the samples was attributed to the inhomogeneity of the sheets. The mechanical properties of the TPS are essential for specifying the purpose and the area of application. A material's capacity to resist the highest possible tensile stress without breaking refers to tensile strength. Young's modulus represents the material's stiffness, whereas elongation at break represents ductility. Tensile strength for the TPS303 is similar to the data reported by Hazar Yoruç & Uğraşkan (2017), while elongation at break is higher and modulus value is lower. The difference in mechanical properties depends on the starch source and processing conditions.

Table 4.2. The mechanical properties of the obtained products.

Product	Tensile Strength (MPa)		Young's Modulus (MPa)		Elongation at Break (%)	
	Average	Standard Deviation	Average	Standard Deviation	Average	Standard Deviation
TPS201	0.64	± 0.32	0.99	± 1.48	8.75	± 3.56
TPS301	4.27	± 0.46	31.41	± 11.21	32.89	± 5.74
TPS302	4.58	± 0.70	25.74	± 7.52	35.25	± 10.15
TPS303	4.83	± 0.23	90.1	± 4.92	58.52	± 19.61
TPS401	3.75	± 0.32	36.87	± 5.45	56.95	± 4.31
TPS402	3.10	± 0.54	21.31	± 4.86	45.21	± 11.26
TPS403	2.51	± 0.32	15.80	± 4.42	56.43	± 13.00
TPSS1	2.81	± 0.64	21.84	± 7.53	32.18	± 9.87
TPSM1	3.63	± 0.11	19.75	± 2.85	84.69	± 3.09

4.3.1. Effect of Pretreatment on Mechanical Properties

4.3.1.1. Effect of Moisture Content on Mechanical Properties

The effect of moisture content on the material's mechanical properties was investigated by comparing the samples TPS301 and TPSM1. Increasing the moisture content decreased tensile strength from 4.27 ± 0.46 MPa to 3.63 ± 0.11 MPa and Young's

modulus from 31.41 ± 11.21 to 19.75 ± 2.85 MPa but increased elongation at break from 32.89% ± 5.74 to 84.69% ± 3.09. Previous studies also reported a similar trend (Janssen & Moscicki, 2009; Mohammadi Nafchi et al., 2013). Moisture acts as a plasticizer, decreasing the molecular interaction between starch molecules, decreasing tensile strength and Young's modulus, and increasing elongation at break.

4.3.1.2. Effect of Sieving on Mechanical Properties

The effect of sieving on the mechanical properties was investigated by comparing the samples TPS301 and TPSS1. The tensile strength decreased from 4.27 ± 0.46 MPa to 2.81 ± 0.64 MPa, and Young's modulus from 31.41 ± 11.21 to 21.84 ± 7.53 MPa with increasing mesh size of the sieve. However, elongation at break did not significantly change. Most probably the presence of contaminants resulted in a greener product color and lower mechanical properties. Since microbial activity and mold formation in the storage occurred and lower mechanical properties were obtained for the starch sieved with 300μm mesh size, using 131μm mesh size was selected as the preferable sieving option.

4.3.2. Effect of Glycerol Content on Mechanical Properties

Fig. 4.9. shows the effect of glycerol content on the average tensile strength of the samples. The tensile strength was the highest for 30 wt.% glycerol (4.56 ± 0.46 MPa) and decreased with increasing to 40 wt.% glycerol (3.12 ± 0.39 MPa) as expected. The unexpectedly low tensile strength obtained with 20 wt.% glycerol content was due to operational problems in the extrusion and incomplete plasticization of the starch. The presence of plasticizer molecules decreased the inner hydrogen bonds and starch-starch interaction by penetrating starch granules and replacing them with starch-glycerol interaction. Consequently, the increased free volume and chain mobility lowered the tensile strength.

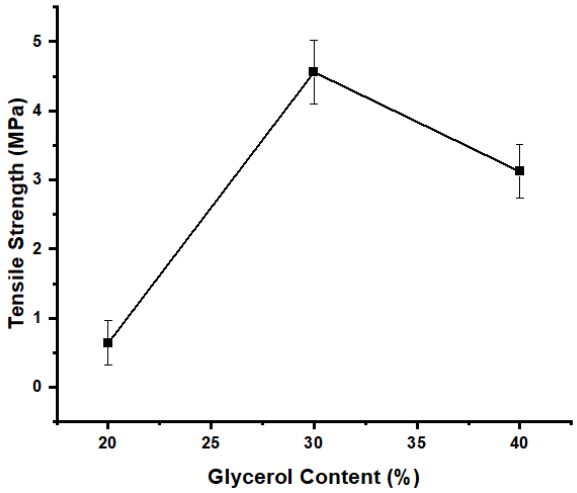

Figure 4.9. The change of average tensile strength with glycerol content.

The average Young's modulus was 0.99 ± 1.48 MPa for 20 wt.% glycerol and increased to 49.08 ± 7.88 MPa for 30 wt.% glycerol and 24.66 ± 4.91 MPa for 40 wt.% glycerol, as shown in Fig. 4.10. The Young's modulus decreased with increasing glycerol content from 30 to 40 wt.%, as expected. The lowest Young's modulus, obtained for 20 wt.% glycerol content suggests the lowest stiffness of the material obtained due to the lower substantial molecular interaction between starch molecules (Yu et al., 1996, 1998).

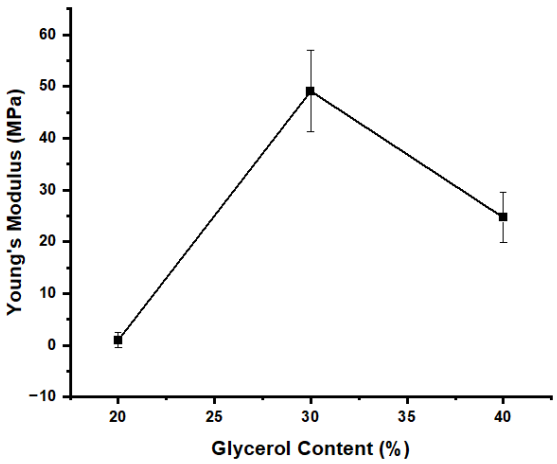

Figure 4.10. The change of average Young's modulus with glycerol content.

The effect of glycerol content on average elongation at break was shown in Fig. 4.11. The average elongation at break values increased from 8.75% ± 3.56 for 20 wt.% glycerol to 52.86% ± 9.52 for 40 wt.% glycerol. The increase in the elongation at break

with the increased glycerol amounts was due to enhanced chain mobility as a result of the penetration of glycerol between the chains (Yu et al., 1996, 1998).

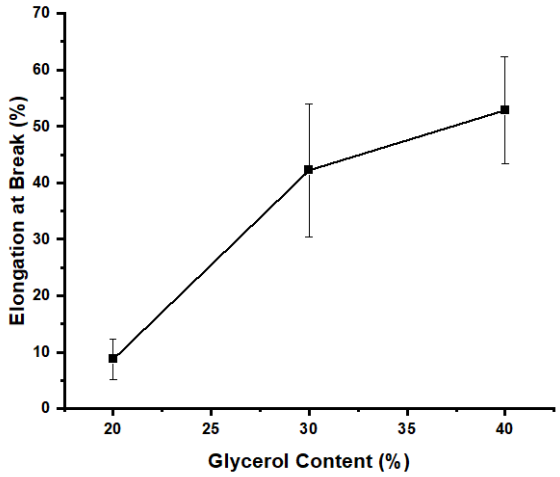

Figure 4.11. The change of average elongation at break with glycerol content.

4.3.3. Effect of Temperature on Mechanical Properties

Fig. 4.12. shows the effect of temperature on tensile strength with different glycerol contents. For 40 wt.% glycerol content, tensile strength decreased from 3.75 ± 0.32 MPa to 2.51 ± 0.32 MPa as the initial zone temperature was raised from 50 to 70°C. However, tensile strength increased from 4.27 ± 0.46 to 4.83 ± 0.23 with increasing initial zone temperature for 30 wt.% glycerol content. The results suggest that increasing temperature could affect the tensile strength differently depending on the glycerol amount. According to the study of Pushpadass et al. (2008), the effect of extrusion temperature on the tensile properties of starch films were found insignificant and inconclusive due to the variations in the thickness of the obtained films. However, the type and concentration of the plasticizer significantly affected the mechanical properties. Zakaria et al. (2018) reported that mixing temperature affected the mechanical properties of potato starch films. The tensile strength of the starch film was increased from 2 MPa to 2.6 MPa with increasing temperature from 80 to 85°C; however, a further increase to 90°C decreased tensile strength to 2.5 MPa, which was attributed to structural changes. They claimed that increasing mixing temperature changed the matrix of the film to a less dense form, resulting in lower tensile strength.

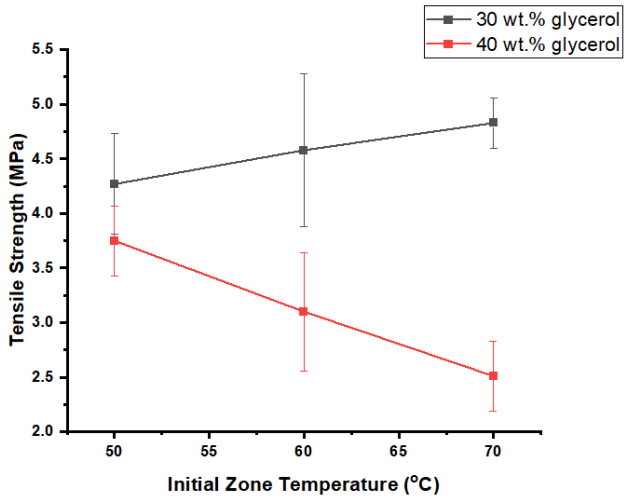

Figure 4.12. The change of tensile strength with temperature sets for different glycerol contents.

The effect of temperature on Young's modulus with different glycerol contents was shown in Fig. 4.13. The Young's modulus of the samples containing 40 wt.% glycerol decreased from 36.87 ± 5.45 MPa to 15.80 ± 4.42 MPa by increasing temperature from 50 to 70°C. On the other hand, the samples prepared with 30 wt.% glycerol showed a significant change in their Young's modulus values with increasing temperature to 70°C. The Young's modulus increased from 31.41 ± 11.21 to 90.1 ± 4.92 MPa with increasing temperature from 50 to 70°C. The higher tensile strength and Young's modulus values with increasing extrusion temperature were attributed to the change in material's crystallinity with more amylose and amylopectin leaching out of granules.

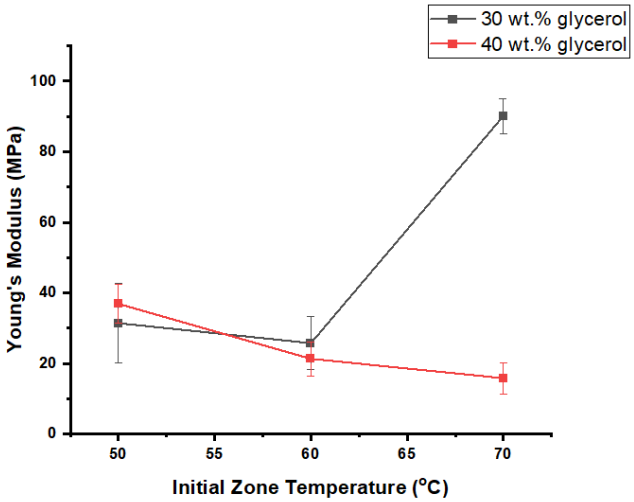

Figure 4.13. The change of Young's modulus with temperature sets for different glycerol contents.

The elongation at break values of the samples containing 30 wt.% glycerol increased from 32.89% ± 5.74 at 50°C to 58.52% ± 19.61 when the temperature was raised to 70°C, as shown in Fig. 4.14. However, samples prepared with 40 wt.% glycerol did not display a significant change in the elongation with temperature.

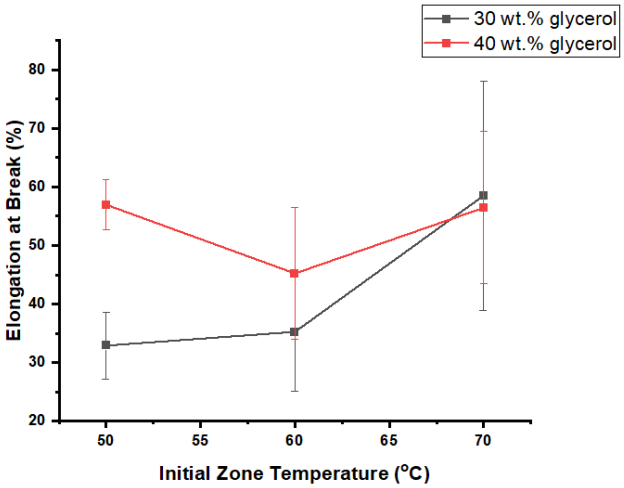

Figure 4.14. The change of elongation at break with temperature sets for different glycerol contents.

4.4. XRD (X-Ray diffraction analysis) Analysis of the Extrudates

The effect of glycerol content and the initial zone temperature in the extruder on the crystallinity of the samples was investigated with the XRD patterns, as shown in Fig. 4.15. The samples, TPS 301 and TPS 402, are partially crystalline, while the structure of TPS401 was found to be amorphous without diffraction peaks. The XRD pattern for TPS402 was similar to the work of Abd Karim et al. (2022) and Mb et al. (2013). The major peaks were observed at the 2θ angle near 17° and 20°, which suggests B and V-type crystallinity for TPS402. The B-type crystal structure has major peaks at the 2θ value near 16.8° and 17.1°. The V-type crystal structure has two subtypes, which are V_a anhydrous crystal structure (2θ at 13.2° and 20.1°) and V_h hydrated crystal structure (2θ at 12.6° and 19.4°) (Orue et al., 2014; Corradini et al., 2007). For TPS301, there was a slight peak at the 2θ value near 20°, which suggests V-type crystallinity. The crystallinity decreased by increasing glycerol content from 30 to 40 wt.% at the same processing temperature. The crystal structure formation of TPS was attributed to the retrogradation

effect, which occurs due to the intermolecular hydrogen bonding between amylose and amylopectin molecules (Zhang & Rempel, 2012). According to the data, temperature was found to have a more pronounced effect on crystallinity than the glycerol content. When the processing temperature increases, more interaction between the amylose and amylopectin molecules could occur, which results in more crystal structure formation due to retrogradation (Zhang & Rempel, 2012).

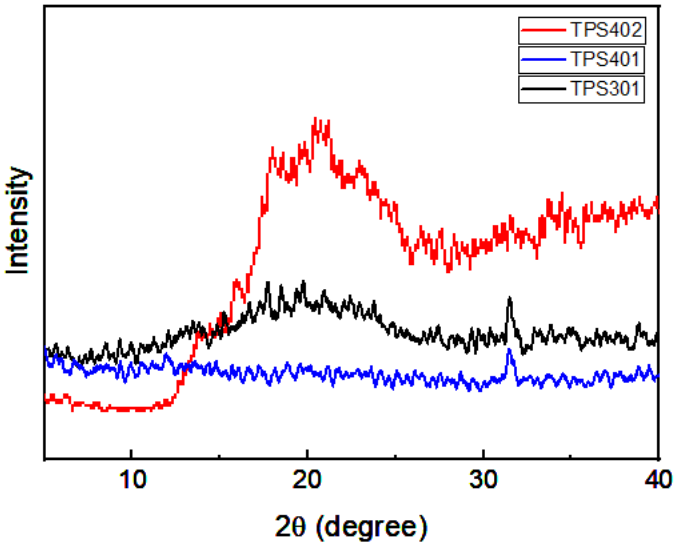

Figure 4.15. XRD patterns of TPS301, TPS401 and TPS402.

4.5. Characterization of the Suggested Product

The optimal glycerol content for the final product was chosen by considering mechanical properties within the range found in the literature. Additionally, it was important to ensure that this chosen content did not lead to the formation of steam bubbles and resulted in the lowest specific mechanical energy consumption. Based on the results, the optimal mechanical properties were achieved when using a glycerol content of 30 wt.%, which contrasted with the literature findings that exhibited a lower Young's modulus and higher elongation at break values. Additionally, the product manufactured with the third temperature set, labeled as TPS303, was selected as the recommended product because it yielded the lowest energy consumption.

4.5.1. SEM (Scanning Electron Microscopy) Analysis

The microstructure of the TPS303, including its homogeneity and surface smoothness, was investigated by SEM analysis, as shown in Fig. 4.16. TPS303 showed inhomogeneous surface morphology and a typical droplet-like structure similar to the work of Jariyasakoolroj & Chirachanchai (2022). The starch granules were observed in the oval shape as characteristic of potato starch. The inhomogeneous surface morphology and the presence of starch grains suggested an incomplete gelatinization process depending on the mixture and processing conditions. The complete degradation of the granules could result in a homogeneous surface. The homogeneous morphology of the thermoplastic starch indicates the structural integrity of the matrix, and it affects the tensile properties of the obtained products (Domene-López et al., 2019).

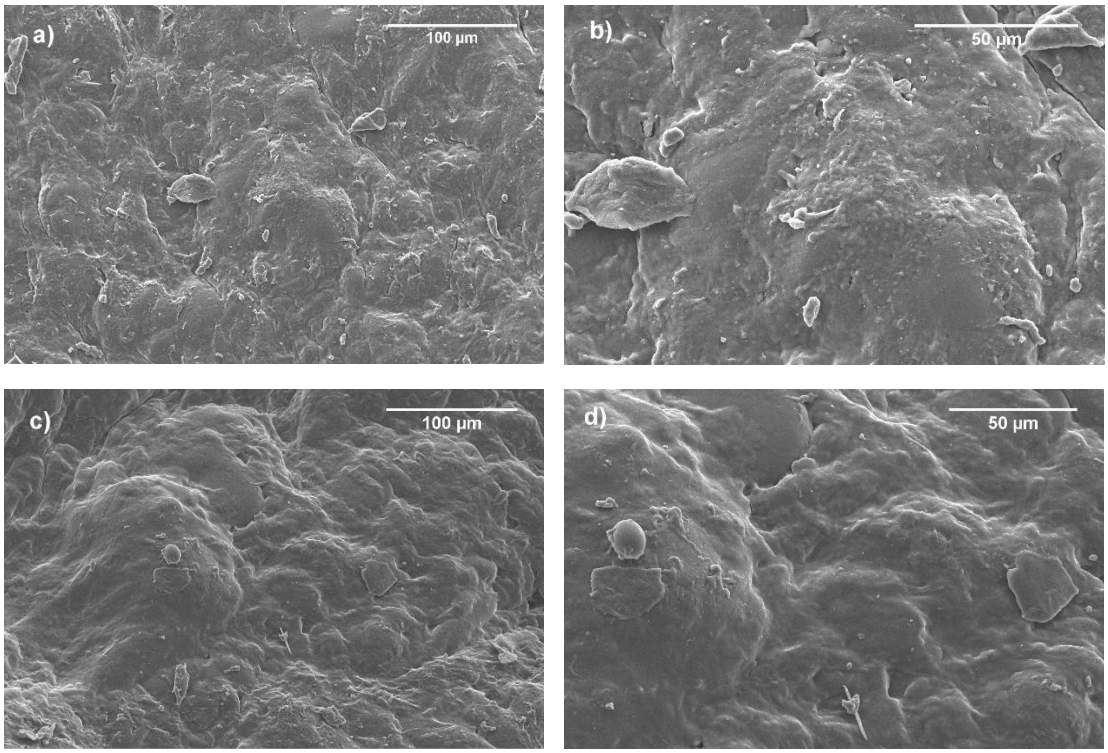

Figure 4.16. SEM images of TPS303 1000 × (a,c), 2000 × (d) and 2500 × (b) magnification.

4.5.2. XRD (X-Ray diffraction analysis) Analysis

The XRD pattern of TPS303 is shown in Fig. 4.17. TPS303 was found to be highly amorphous with a small crystalline fraction. The main peak was observed near 2θ value of 5°, and the slight peaks were observed around 2θ value near 17° and 20°. The peak

formation at 5.5° suggests B-type crystallinity, and the peak at 6.3° indicates Vh-type crystallinity (Dean et al., 2008; Domene-López et al., 2019). The slight peaks near 17° and 20° suggested B and V-type crystal structures. The extruded thermoplastic starch is in amorphous form. The formation of the B-type crystal structure was attributed to the crystallization of the short outer chains of amylopectin. The appearance of a V-type crystal structure was attributed to the crystallization of amylose in single helices involving glycerol (Corradini et al., 2007).

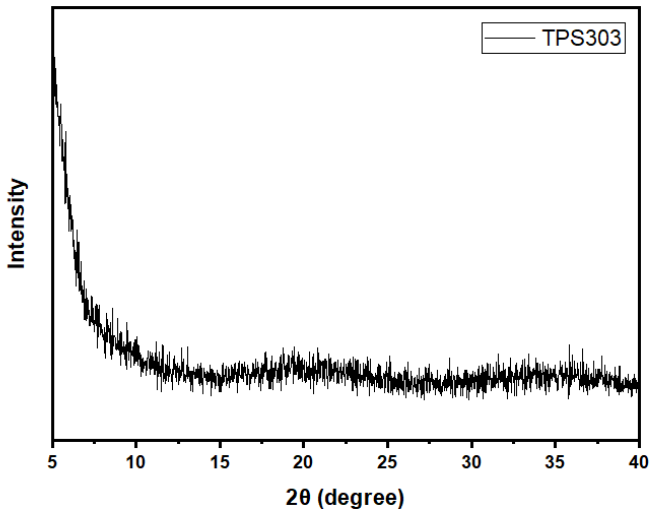

Figure 4.17. XRD pattern of TPS303.

4.5.3. FTIR (Fourier Transform Infrared Spectroscopy) Analysis

The FTIR analysis was conducted to determine the chemical structure and possible starch-plasticizer interactions for pretreated starch, starch + 30 wt.% glycerol mixture, and TPS303, as shown in Fig. 4.18. The absorption peaks were observed in the same regions for starch, starch and 30 wt.% glycerol mixture and TPS303, suggesting identical functional groups. The FTIR pattern of starch was similar to the work of Hejna et al. (2019), and the FTIR pattern of TPS303 was identical to the work of Da Róz et al. (2016). The main overlapping FTIR peaks at 3400-3450 cm^{-1} indicate O-H stretching; 2880-2900 cm^{-1} indicate C-H stretching; 1200-1500 cm^{-1} indicate C-H bending; 900-1200cm^{-1} indicate C-O stretching (Da Róz et al., 2016; Julinová et al., 2019; Turco et al., 2019). The peaks between 800-1000 cm^{-1} indicate C-C stretching, whereas the water absorbed by the amorphous region of the starch was represented by O-H bending at peak

1600 cm^{-1} (Turco et al., 2019; Ma et al., 2018). As expected, the presence of glycerol in the starch sample made the band between 3000-3500 cm^{-1} wider.

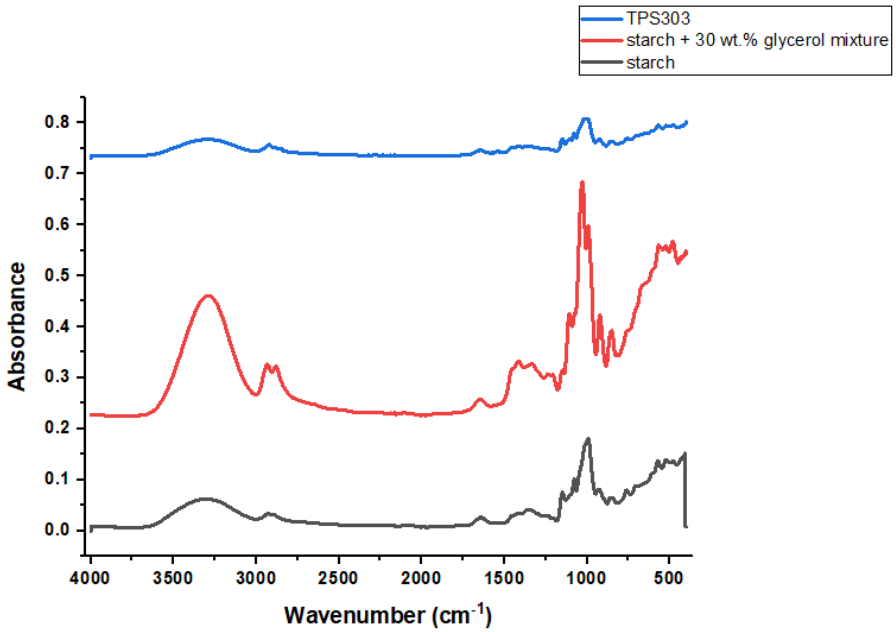

Figure 4.18. FTIR spectra of starch, starch + 30 wt.% glycerol mixture and TPS303.

4.5.4. DSC (Differential Scanning Calorimetry) Analysis

The glass transition temperature of pretreated starch, starch + 30 wt.% glycerol mixture, and TPS303 were estimated by DSC analysis as shown in Fig. 4.19. The T_g of potato starch was estimated as 83°C and decreased to 68°C with the addition of 30 wt.% glycerol. The T_g of TPS303 was estimated as 36°C. Adding a plasticizer and extruding the mixture reduced the glass transition temperature as expected. Since the plasticizer increases the free volume between polymer chains, they slide past one another at lower temperatures. Therefore, the glass transition temperature decreases with the addition of a plasticizer. The glass transition temperature of the mixture depends on the moisture content, amylose to amylopectin ratio of the starch and the glycerol amount (Habitante et al., 2008; Mitrus, 2005). According to the study of Mitrus (2005), increasing glycerol content from 15 to 30 wt.% decreased the T_g of thermoplastic starch from 132 to 18°C with 15 wt.% moisture content.

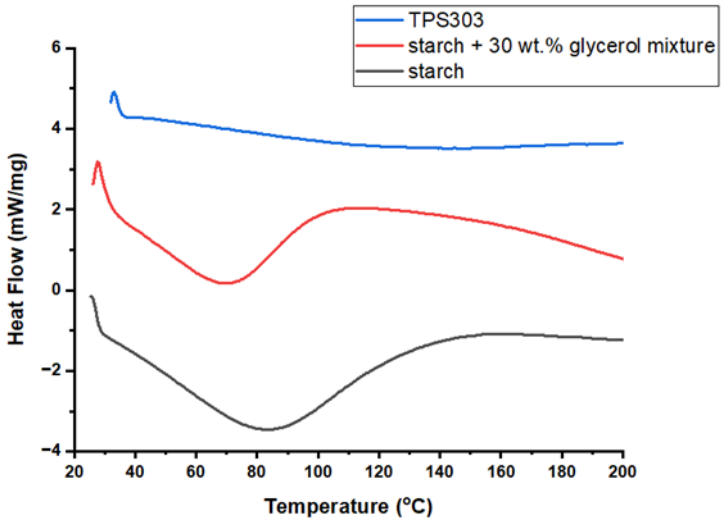

Figure 4.19. DSC curve for starch, starch + 30 wt.% glycerol mixture and TPS303.

CHAPTER 5

CONCLUSION

This thesis studied the production of thermoplastic starch from residual potato starch by extrusion. The source of the potato starch was the production lines of potato chips. The pretreatment of the residual starch was carried out by decreasing the moisture content from 40 to 10 wt.% by drying and sieving the contaminants with a 131µm mesh-sized sieve. Glycerol was used as a plasticizer with 20, 30, and 40 wt.% by starch mass. The feed to the extruder was prepared by mixing pretreated starch with glycerol for two minutes using an electric mixer. Before extrusion, the mixture was stored in an airtight plastic container for three hours to penetrate the plasticizer molecules into starch. The extrusion was carried out in a single screw extruder with four different temperature units. Specific mechanical energy consumption was measured for each trial, and mechanical testing was conducted for the obtained extrudates. The temperature profiles were between 50-90^{o}C, 60-90^{o}C and 70-90^{o}C. Continuous production was impossible for the feed containing 20 wt.% glycerol and processed with the initial zone temperatures of 60^{o}C and 70^{o}C due to steam bubble formation.

The effects of moisture content and sieving with 131µm and 300µm mesh sizes on the mechanical properties of the samples extruded at 30 wt.% glycerol content with a 50-90^{o}C temperature profile were investigated. Increasing starch's moisture content from 10 wt.% to 26 wt.% decreased the specific mechanical energy from 43.27 kWhkg^{-1} to 18.30 kWhkg^{-1}. An increase in the moisture content decreased the tensile strength from 4.27 ± 0.46 MPa to 3.63 ± 0.11 MPa, Young's modulus from 31.41 ± 11.21 MPa to 19.75 ± 2.85 MPa, but increased elongation at break from 32.89% ± 5.74 to 84.69% ± 3.09. Water acts as a plasticizer and decreases the inner hydrogen bonds by acting as a diluent, which decreases tensile strength and Young's modulus and increases elongation at break. 10 wt.% moisture content resulted in better mechanical properties and allowed continuous production without sticking to extruder wall. Starch sieved with 300 µm mesh size was processed with a lower specific mechanical energy consumption than 131 µm mesh size sieved starch. However, sieving with a 300 µm mesh size decreased tensile strength from 4.27 ± 0.46 MPa to 2.81 ± 0.64 MPa and Young's modulus from 31.41 ± 11.21 MPa to

21.84 ± 7.53 MPa; additionally, microbial activity and mold formation were observed. Sieving with a 131µm mesh size was more suitable for removing impurities from residual starch. The amount of glycerol content was found to be an important parameter for continuous production. Adding more glycerol decreases the mixture's viscosity and lowers the SME from 30.42 $kWhkg^{-1}$ for 30 wt.% glycerol to 3.82 $kWhkg^{-1}$ for 40 wt.% glycerol contents. Similarly, increasing the initial zone temperature for both glycerol contents reduced the viscosity of the solution and decreased the SME consumption values. For 40 wt.% glycerol content, tensile strength decreased from 3.75 ± 0.32 MPa to 2.51 ± 0.32 MPa, Young's modulus from 36.87 ± 5.45 MPa to 15.80 ± 4.42 MPa, while elongation at break values did not significantly change by increasing initial zone temperature from 50°C to 70°C. Within the same temperature increase, the tensile strength of the samples containing 30 wt.% glycerol did not change, Young's modulus increased from 31.41 ± 11.21 MPa to 90.1 ± 4.92 MPa, and the elongation at break increased from 32.89% ± 5.74 to 58.52% ± 19.61. The XRD patterns obtained for TPS301, TPS401, and TPS402 suggest that the samples' crystallinity depends on the extruder's initial zone temperature.

To conclude, residual potato starch was found to be a promising waste material for thermoplastic starch production with proper pretreatment. The optimum pretreatment conditions for residual potato starch were selected as drying to 10 wt.% moisture content level and sieving with 131µm mesh size. The 30 wt.% glycerol content exhibited optimum mechanical properties compared to the literature. Since the lowest energy consumption was observed for the initial zone temperature of 70°C, TPS303 was selected as the optimum product. Nevertheless, depending on the application area, it is possible to adjust the mechanical properties of the TPS.

REFERENCES

Abd Karim, S. F.; Idris, J.; Jai, J.; Musa, M.; Ku Hamid, K. H. Production of Thermoplastic Starch-Aloe Vera Gel Film with High Tensile Strength and Improved Water Solubility. *Polymers* **2022**, *14* (19), 4213. DOI:10.3390/polym14194213.

Administrador-AC. Zinc Stearate: Other Chemicals. https://www.adplast.pt/products-en/other-chemicals/zinc-stearate/ (accessed 2023-10-10).

Arboleda, G. A.; Montilla, C. E.; Villada, H. S.; Varona, G. A. Obtaining a Flexible Film Elaborated from Cassava Thermoplastic Starch and Polylactic Acid. *International Journal of Polymer Science* **2015**, 1–9. DOI:10.1155/2015/627268.

Ayala, G.; Vargas, R. A.; Agudelo, A. C. Influence of Glycerol and Temperature on the Rheological Properties of Potato Starch Solutions. *International Agrophysics* **2014**, *28* (3), 261–268. DOI:10.2478/intag-2014-0016.

Bindzus, W.; Livings, S. J.; Gloria-Hernandez, H.; Fayard, G.; van Lengerich, B.; Meuser, F. Glass Transition of Extruded Wheat, Corn and Rice Starch. *Starch - Stärke* **2002**, *54* (9), 393–400. DOI:10.1002/1521-379x(200209)54:9<393::aid-star393>3.0.co;2-w.

Bîrcă, A.; Gherasim, O.; Grumezescu, V.; Grumezescu, A. M. Introduction in Thermoplastic and Thermosetting Polymers. *Materials for Biomedical Engineering* **2019**, 1–28. DOI:10.1016/b978-0-12-816874-5.00001-3.

BIOTEC. Advanced Biopolymers for Building a Better Tomorrow. https://www.biotec.de/ (accessed 2023-10-10).

Brümmer, T.; Meuser, F.; van Lengerich, B.; Niemann, C. Effect of Extrusion Cooking on Molecular Parameters of Corn Starch. *Starch - Stärke* **2002**, *54* (1), 1–8. DOI:10.1002/1521-379x(200201)54:1<1::aid-star1>3.0.co;2-9.

Carvalho, C. W. P.; Takeiti, C. Y.; Onwulata, C. I.; Pordesimo, L. O. Relative Effect of Particle Size on the Physical Properties of Corn Meal Extrudates: Effect of Particle Size on the Extrusion of Corn Meal. *Journal of Food Engineering* **2010**, *98* (1), 103–109. DOI:10.1016/j.jfoodeng.2009.12.015.

Cazón, P.; Velazquez, G.; Ramírez, J. A.; Vázquez, M. Polysaccharide-Based Films and Coatings for Food Packaging: A Review. *Food Hydrocolloids* **2017**, *68*, 136–148. DOI:10.1016/j.foodhyd.2016.09.009.

Charles, A. L.; Motsa, N.; Abdillah, A. A. A Comprehensive Characterization of Biodegradable Edible Films Based on Potato Peel Starch Plasticized with Glycerol. *Polymers* **2022**, *14* (17), 3462. DOI:10.3390/polym14173462.

ChemAnalyst. Glycerine Market Analysis: Industry Market Size, Plant Capacity, Production, Operating Efficiency, Demand & Supply, End-User Industries, Foreign Trade, Sales Channel, Regional Demand, Company Share, 2015-2030. https://www.chemanalyst.com/industry-report/glycerine-market-635 (accessed 2023-10-10).

Christoph, R.; Schmidt, B.; Steinberner, U.; Dilla, W.; Karinen, R. Glycerol. *Ullmann's Encyclopedia of Industrial Chemistry* **2006**. DOI:10.1002/14356007.a12_477.pub2.

Combrzyński, M.; Matwijczuk, A.; Wójtowicz, A.; Oniszczuk, T.; Karcz, D.; Szponar, J.; Niemczynowicz, A.; Bober, D.; Mitrus, M.; Kupryaniuk, K.; Stasiak, M.; Dobrzański, B.; Oniszczuk, A. Potato Starch Utilization in Ecological Loose-Fill Packaging Materials—Sustainability and Characterization. *Materials* **2020**, *13* (6), 1390. DOI:10.3390/ma13061390.

Combrzyński, M., Mitrus, M., Mościcki., L., Oniszczuk, T., & Wójtowicz, A. Selected Aspects of Thermoplastic Starch Production. *TEKA Commission of Motorization and Power Industry in Agriculture* **2012**, *12* (1), 25–29.

Corradini, E.; Carvalho, A. J.; Curvelo, A. A.; Agnelli, J. A.; Mattoso, L. H. Preparation and Characterization of Thermoplastic Starch/Zein Blends. *Materials Research* **2007**, *10* (3), 227–231. DOI:10.1590/s1516-14392007000300002.

Da Róz, A. L.; Veiga-Santos, P.; Ferreira, A. M.; Antunes, T. C.; Leite, F. de; Yamaji, F. M.; Carvalho, A. J. Water Susceptibility and Mechanical Properties of Thermoplastic Starch–Pectin Blends Reactively Extruded with Edible Citric Acid. *Materials Research* **2016**, *19* (1), 138–142. DOI:10.1590/1980-5373-mr-2015-0215.

Das, M. Effect of Screw Speed and Plasticizer on the Torque Requirement in Single Screw Extrusion of Starch-Based Plastics and Their Mechanical Properties. Indian Journal of Chemical Technology **2008**, 555–559.

De Graaf, R. A.; Karman, A. P.; Janssen, L. P. Material Properties and Glass Transition Temperatures of Different Thermoplastic Starches after Extrusion Processing. *Starch - Stärke* **2003**, *55* (2), 80–86. DOI:10.1002/star.200390020.

Dean, K. M.; Do, M. D.; Petinakis, E.; Yu, L. Key Interactions in Biodegradable Thermoplastic Starch/Poly(Vinyl Alcohol)/Montmorillonite Micro- and Nanocomposites. *Composites Science and Technology* **2008**, *68* (6), 1453–1462. DOI:10.1016/j.compscitech.2007.10.037.

Dilkes-Hoffman, L.; Ashworth, P.; Laycock, B.; Pratt, S.; Lant, P. Public Attitudes towards Bioplastics – Knowledge, Perception and End-of-Life Management. *Resources, Conservation and Recycling* **2019**, *151*, 104479. DOI:10.1016/j.resconrec.2019.104479.

Dobrucka, R. Bioplastic Packaging Materials in Circular Economy. *Logforum* **2019**, *15* (1), 129–137. DOI:10.17270/j.log.2019.322.

Domene-López, D.; García-Quesada, J. C.; Martin-Gullon, I.; Montalbán, M. G. Influence of Starch Composition and Molecular Weight on Physicochemical Properties of Biodegradable Films. *Polymers* **2019**, *11* (7), 1084. DOI:10.3390/polym11071084.

Emadian, S. M.; Onay, T. T.; Demirel, B. Biodegradation of Bioplastics in Natural Environments. *Waste Management* **2017**, *59*, 526–536. DOI:10.1016/j.wasman.2016.10.006.

European Bioplastics. https://www.european-bioplastics.org/market/ (accessed 2023-10-10).

Forssell, P. M.; Mikkilä, J. M.; Moates, G. K.; Parker, R. Phase and Glass Transition Behaviour of Concentrated Barley Starch-Glycerol-Water Mixtures, a Model for Thermoplastic Starch. *Carbohydrate Polymers* **1997**, *34* (4), 275–282. DOI:10.1016/s0144-8617(97)00133-1.

González-Seligra, P.; Guz, L.; Ochoa-Yepes, O.; Goyanes, S.; Famá, L. Influence of Extrusion Process Conditions on Starch Film Morphology. *LWT* **2017**, *84*, 520–528. DOI:10.1016/j.lwt.2017.06.027.

Halley, P. J.; Dorgan, J. R. Next-Generation Biopolymers: Advanced Functionality and Improved Sustainability. *MRS Bulletin* **2011**, *36* (9), 687–691. DOI:10.1557/mrs.2011.180.

Hazar Yoruç, A. B.; Uğraşkan, V. Green Polymers and Applications. *Afyon Kocatepe University Journal of Sciences and Engineering* **2017**, *17* (1), 318–337. DOI:10.5578/fmbd.53940.

Hejna, A.; Lenża, J.; Formela, K.; Korol, J. Studies on the Combined Impact of Starch Source and Multiple Processing on Selected Properties of Thermoplastic Starch/Ethylene-Vinyl Acetate Blends. *Journal of Polymers and the Environment* **2019**, *27* (5), 1112–1126. DOI:10.1007/s10924-019-01406-1.

Hoover, R. Composition, Molecular Structure, and Physicochemical Properties of Tuber and Root Starches: A Review. *Carbohydrate Polymers* **2001**, *45* (3), 253–267. DOI:10.1016/s0144-8617(00)00260-5.

Hulleman, S. H. D.; Janssen, F. H. P.; Feil, H. The Role of Water during Plasticization of Native Starches. *Polymer* **1998**, *39* (10), 2043–2048. DOI:10.1016/s0032-3861(97)00301-7.

Janssen, L.P.B.M., Mościcki, L., Mitrus, M. Energy aspects in food extrusion-cooking. International Agrophysics. International Agrophysics **2002**, *16*, 191-195.

Janssen, L. L. B. M.; Moscicki, L. *Thermoplastic Starch: A Green Material for Various Industries*; Wiley-VCH, 2009.

Jariyasakoolroj, P.; Chirachanchai, S. In Situ Chemical Modification of Thermoplastic Starch with Poly(L-Lactide) and Poly(Butylene Succinate) for an Effectively

Miscible Ternary Blend. *Polymers* **2022**, *14* (4), 825. DOI:10.3390/polym14040825.

Jõgi, K.; Bhat, R. Valorization of Food Processing Wastes and By-Products for Bioplastic Production. *Sustainable Chemistry and Pharmacy* **2020**, *18*, 100326. DOI:10.1016/j.scp.2020.100326.

Julinová, M.; Vaňharová, L.; Jurča, M.; Minařík, A.; Duchek, P.; Kavečková, J.; Rouchalová, D.; Skácelík, P. Effect of Different Fillers on the Biodegradation Rate of Thermoplastic Starch in Water and Soil Environments. *Journal of Polymers and the Environment* **2019**, *28* (2), 566–583. DOI:10.1007/s10924-019-01624-7.

Karan, H.; Funk, C.; Grabert, M.; Oey, M.; Hankamer, B. Green Bioplastics as Part of a Circular Bioeconomy. *Trends in Plant Science* **2019**, *24* (3), 237–249. DOI:10.1016/j.tplants.2018.11.010.

Kaseem, M.; Hamad, K.; Deri, F. Thermoplastic Starch Blends: A Review of Recent Works. *Polymer Science Series A* **2012**, *54* (2), 165–176. DOI:10.1134/s0965545x1202006x.

Khan, B.; Bilal Khan Niazi, M.; Samin, G.; Jahan, Z. Thermoplastic Starch: A Possible Biodegradable Food Packaging Material—a Review. *Journal of Food Process Engineering* **2016**, *40* (3). DOI:10.1111/jfpe.12447.

Laftah, W. A. Starch Based Biodegradable Blends: A Review. *International journal of engineering research and technology* **2017**, *6*.

Levine, L. More on Extruder Energy Balances. *Cereal Foods World*, **1997**, *42*, 772.

Lizarazo H., S. P.; Hurtado R., G. G.; Rodríguez, L. F. Physicochemical and Morphological Characterization of Potato Starch (Solanum Tuberosum L.) as Raw Material for the Purpose of Obtaining Bioethanol. *Agronomía Colombiana* **2015**, *33* (2), 244–252. DOI:10.15446/agron.colomb.v33n2.47239.

Lu, D. R.; Xiao, C. M.; Xu, S. J. Starch-Based Completely Biodegradable Polymer Materials. *Express Polymer Letters* **2009**, *3* (6), 366–375. DOI:10.3144/expresspolymlett.2009.46.

Ma, Q.; Dutta, S.; Wu, K. C. -W.; Kimura, T. Analytical Understanding of the Materials Design with Well-described Shrinkages on Multiscale. *Chemistry – A European Journal* **2018**, *24* (27), 6886–6904. DOI:10.1002/chem.201704198.

Mali, S.; Grossmann, M. V.; García, M. A.; Martino, M. N.; Zaritzky, N. E. Mechanical and Thermal Properties of Yam Starch Films. *Food Hydrocolloids* **2005**, *19* (1), 157–164. DOI:10.1016/j.foodhyd.2004.05.002.

Mb, M., Mj, Y., Tj, K., Eg, K., Us, I., Mk, Y., & Dj, W. Characterization and Thermomechanical Properties of Thermoplastic Potato Starch. *Research & Reviews: Journal of Engineering and Technology* **2013**, *2*, 9–16.

Mehyar, G. F.; Han, J. H. Physical and Mechanical Properties of High-Amylose Rice and Pea Starch Films as Affected by Relative Humidity and Plasticizer. *Journal of Food Science* **2006**, *69* (9). DOI:10.1111/j.1365-2621.2004.tb09929.x.

Mitrus, Marcin. Glass Transition Temperature of Thermoplastic Starches. *International Agrophysics* **2005**, *19*, 237–241.

Mitrus, M., Oniszczuk, T. and Mościcki, L. Changes of Specific Mechanical Energy During Extrusion-Cooking of Potato Starch. *TEKA Kom. Mot. i Energ. Roln* **2011**, *11*, 152–157.

Mitrus, M., & Mooecicki, L. Physical properties of thermoplastic starches. *International Agrophysics* **2009**, *23*, 305–308.

Montilla-Buitrago, C. E.; Gómez-López, R. A.; Solanilla-Duque, J. F.; Serna-Cock, L.; Villada-Castillo, H. S. Effect of Plasticizers on Properties, Retrogradation, and Processing of Extrusion-obtained Thermoplastic Starch: A Review. *Starch - Stärke* **2021**, *73* (9–10). DOI:10.1002/star.202100060.

Mohammadi Nafchi, A.; Moradpour, M.; Saeidi, M.; Alias, A. K. Thermoplastic Starches: Properties, Challenges, and Prospects. *Starch - Stärke* **2013**, *65* (1–2), 61–72. DOI:10.1002/star.201200201.

Ochoa-Yepes, O.; Di Giogio, L.; Goyanes, S.; Mauri, A.; Famá, L. Influence of Process (Extrusion/Thermo-Compression, Casting) and Lentil Protein Content on Physicochemical Properties of Starch Films. *Carbohydrate Polymers* **2019**, *208*, 221–231. DOI:10.1016/j.carbpol.2018.12.030.

Oniszczuk, T.; Wójtowicz, A.; Oniszczuk, A.; Mitrus, M.; Combrzyński, M.; Kręcisz, M.; Mościcki, L. Effect of Processing Conditions on Selected Properties of Starch-Based Biopolymers. *Agriculture and Agricultural Science Procedia* **2015**, *7*, 192–197. DOI:10.1016/j.aaspro.2015.12.016.

Orue, A.; Corcuera, M. A.; Peña, C.; Eceiza, A.; Arbelaiz, A. Bionanocomposites Based on Thermoplastic Starch and Cellulose Nanofibers. *Journal of Thermoplastic Composite Materials* **2014**, *29* (6), 817–832. DOI:10.1177/0892705714536424.

Pushpadass, H. A.; Marx, D. B.; Hanna, M. A. Effects of Extrusion Temperature and Plasticizers on the Physical and Functional Properties of Starch Films. *Starch - Stärke* **2008**, *60* (10), 527–538. DOI:10.1002/star.200800713.

Rosenboom, J.-G.; Langer, R.; Traverso, G. Bioplastics for a Circular Economy. *Nature Reviews Materials* **2022**, *7* (2), 117–137. DOI:10.1038/s41578-021-00407-8.

Schulze, C.; Juraschek, M.; Herrmann, C.; Thiede, S. Energy Analysis of Bioplastics Processing. *Procedia CIRP* **2017**, *61*, 600–605. DOI:10.1016/j.procir.2016.11.181.

Shen, L., Haufe, J., & Patel, M.K. *Product Overview and Market Projection of Emerging Bio-Based Plastics*; PRO-BIP: The Netherlands, June 2009.

Shogren, R. L. Effect of Moisture Content on the Melting and Subsequent Physical Aging of Cornstarch. *Carbohydrate Polymers* **1992**, *19* (2), 83–90. DOI:10.1016/0144-8617(92)90117-9.

Singh, A. A.; Genovese, M. E. Green and Sustainable Packaging Materials Using Thermoplastic Starch. *Sustainable Food Packaging Technology* **2021**, 133–160. DOI:10.1002/9783527820078.ch5.

Song, J. H.; Murphy, R. J.; Narayan, R.; Davies, G. B. Biodegradable and Compostable Alternatives to Conventional Plastics. *Philosophical Transactions of the Royal Society B: Biological Sciences* **2009**, *364* (1526), 2127–2139. DOI:10.1098/rstb.2008.0289.

Choi, C. S.; Befroy, D. E.; Codella, R.; Kim, S.; Reznick, R. M.; Hwang, Y.-J.; Liu, Z.-X.; Lee, H.-Y.; Distefano, A.; Samuel, V. T.; Zhang, D.; Cline, G. W.; Handschin, C.; Lin, J.; Petersen, K. F.; Spiegelman, B. M.; Shulman, G. I. Paradoxical Effects of Increased Expression of Pgc-1α on Muscle Mitochondrial Function and Insulin-Stimulated Muscle Glucose Metabolism. *Proceedings of the National Academy of Sciences* **2008**, *105* (50), 19926–19931. DOI:10.1073/pnas.0810339105.

Su, B.; Xie, F.; Li, M.; Corrigan, P. A.; Yu, L.; Li, X.; Chen, L. Extrusion Processing of Starch Film. *International Journal of Food Engineering* **2009**, *5* (1). DOI:10.2202/1556-3758.1617.

Tharanathan, R. N. Biodegradable Films and Composite Coatings: Past, Present and Future. *Trends in Food Science & Technology* **2003**, *14* (3), 71–78. DOI:10.1016/s0924-2244(02)00280-7.

Thuwall, M.; Boldizar, A.; Rigdahl, M. Extrusion Processing of High Amylose Potato Starch Materials. *Carbohydrate Polymers* **2006**, *65* (4), 441–446. DOI:10.1016/j.carbpol.2006.01.033.

Turco, R.; Ortega-Toro, R.; Tesser, R.; Mallardo, S.; Collazo-Bigliardi, S.; Chiralt Boix, A.; Malinconico, M.; Rippa, M.; Di Serio, M.; Santagata, G. Poly (Lactic Acid)/Thermoplastic Starch Films: Effect of Cardoon Seed Epoxidized Oil on Their Chemicophysical, Mechanical, and Barrier Properties. *Coatings* **2019**, *9* (9), 574. DOI:10.3390/coatings9090574.

Valle, G. D.; Boché, Y.; Colonna, P.; Vergnes, B. The Extrusion Behaviour of Potato Starch. *Carbohydrate Polymers* **1995**, *28* (3), 255–264. DOI:10.1016/0144-8617(95)00111-5.

Van Soest, J. J.; Borger, D. B. Structure and Properties of Compression-Molded Thermoplastic Starch Materials from Normal and High-Amylose Maize Starches. *Journal of Applied Polymer Science* **1997**, *64* (4), 631–644. DOI:10.1002/(sici)1097-4628(19970425)64:4<631::aid-app2>3.0.co;2-o.

Xie, F.; Halley, P. J.; Avérous, L. Rheology to Understand and Optimize Processibility, Structures and Properties of Starch Polymeric Materials. *Progress in Polymer Science* **2012**, *37* (4), 595–623. DOI:10.1016/j.progpolymsci.2011.07.002.

Xie, F.; Liu, P.; Yu, L. Processing of Plasticized Starch-Based Materials. *Starch Polymers* **2014**, 257–289. DOI:10.1016/b978-0-444-53730-0.00024-5.

Xie, F.; Luckman, P.; Milne, J.; McDonald, L.; Young, C.; Tu, C. Y.; Pasquale, T. D.; Faveere, R.; Halley, P. J. Thermoplastic Starch. *Journal of Renewable Materials* **2014**, *2* (2), 95–106. DOI:10.7569/jrm.2014.634104.

Yu, J.; Chen, S.; Gao, J.; Zheng, H.; Zhang, J.; Lin, T. A Study on the Properties of Starch/Glycerine Blend. *Starch - Stärke* **1998**, *50* (6), 246–250. DOI:10.1002/(sici)1521-379x(199806)50:6<246::aid-star246>3.0.co;2-7.

Yu, J., Gao, J., & Lin, T. Biodegradable thermoplastic starch. *Journal of Applied Polymer Science* **1996**, *62* (9), 1491–1494. DOI:10.1002/(sici)1097-4628(19961128)62:9<1491::aid-app19>3.0.co;2-1

Zakaria, N. H.; Muhammad, N.; Sandu, A. V.; Abdullah, M. M. Effect of Mixing Temperature on Characteristics of Thermoplastic Potato Starch Film. *IOP Conference Series: Materials Science and Engineering* **2018**, *374*, 012083. DOI:10.1088/1757-899x/374/1/012083.

Zhang, Y.; Rempel, C. Retrogradation and Antiplasticization of Thermoplastic Starch. *Thermoplastic Elastomers* **2012**. DOI:10.5772/35848.

Zhang, Y.; Rempel, C.; Liu, Q. Thermoplastic Starch Processing and Characteristics—a Review. *Critical Reviews in Food Science and Nutrition* **2014**, *54* (10), 1353–1370. DOI:10.1080/10408398.2011.636156.

Ziccardi, L. M.; Edgington, A.; Hentz, K.; Kulacki, K. J.; Kane Driscoll, S. Microplastics as Vectors for Bioaccumulation of Hydrophobic Organic Chemicals in the Marine Environment: A State-of-the-science Review. *Environmental Toxicology and Chemistry* **2016**, *35* (7), 1667–1676. DOI:10.1002/etc.3461.